

COMPUTATION OF VISCOUS FLOWS OVER AIRFOILS
INCLUDING SEPARATION, WITH A COUPLING APPROACH

J. C. LeBalleur

NASA-TM-77079 19840015539

Translation of "Calcul des écoulements à forte interaction visqueuse au moyen de méthodes de couplage," in Computation of Viscous-Inviscid Interaction, Feb. 1981., Symposium held at Colorado Springs, Colo. Sept. 29-Oct 1, 1980, Advisory Group for Aerospace Research and Development, Paris (France), (AGARD-CP-291). 36 pages.

FOR REFERENCE

NOT TO BE TAKEN FROM THIS FILE

MAY 2 1981
LANGLEY RESEARCH CENTER
LIBRARY, BLDG
HAMPTON, VIRGINIA

NATIONAL AERONAUTICS AND SPACE ADMINISTRATION
WASHINGTON D.C. 20546

JUNE 1983



NF00303

STANDARD TITLE PAGE

1. Report No. NASA TM-77079	2. Government Accession No.	3. Recipient's Catalog No.	
4. Title and Subtitle COMPUTATION OF VISCOUS FLOWS OVER AIRFOILS, INCLUDING SEPARATION, WITH A COUPLING APPROACH.		5. Report Date June 1983	
		6. Performing Organization Code	
7. Author(s) J.C. LeBalleur		8. Performing Organization Report No.	
		10. Work Unit No.	
9. Performing Organization Name and Address Leo Kanner Associates, Redwood City, CA 93924		11. Contract or Grant No. NASW-3541	
		13. Type of Report and Period Covered Translation	
12. Sponsoring Agency Name and Address National Aeronautics and Space Administra- tion, Washington, D.C. 20546		14. Sponsoring Agency Code	
15. Supplementary Notes Translation of "Calcul des écoulements à forte interaction visqueuse au moyen de méthodes de couplage," in <u>Computation of Viscous-Inviscid Interaction</u> , Feb. 1981., Symposium held at Colorado Springs, Colo. Sept. 29-Oct. 1, 1980, Advisory Group for Aerospace Research and Development, Paris (France), (AGARD-CP-291) 36 pages. (N81-26048)			
16. Abstract The approximation levels and concepts are outlined, as well as the generalized formulations of the viscous displacement for inviscid flow. The strongly interacting methods that are based on thin viscous layers approximations are discussed. At match- ing formulation of the viscous flow, calculated as a difference of the inviscid overlaying flow, is presented in order to ap- proximate the normal pressure gradient inside of the layers, as well as to eliminate the supercritical behaviors, in the Crocco- Lees sense. This analysis uses simple viscous integral equa- tions. Numerical techniques presently available for the coup- ling problem are reviewed. Results are presented for trailing edge separation, and an approximation method is presented to numerically analyze the viscous interaction under shock waves.			
17. Key Words (Selected by Author(s)) FOR REFERENCE		18. Distribution Statement Unclassified-Unlimited	
19. Security Classif. (of this report) Unclassified	20. Security Classif. (of this page) Unclassified	21. No. of Pages	22.

N-153,930
N84-23607#
N81-26048 (ORIGINAL)

ABSTRACT

The calculation of viscous flows with coupling methods is surveyed. The approximation levels and concepts are first outlined, as well as the generalized formulations of the viscous displacement over the inviscid flow. Then, the strongly interacting methods that are based on thin viscous layers approximations are discussed.

In this way, a matching formulation of the viscous flow, calculated as a difference with the inviscid overlaying flow, is suggested, in order to restore approximately the normal pressure gradient inside of the layers, as well as to remove the supercritical behaviors, in the Crocco-Lees sense. This analysis maintains simple viscous integral equations. A review is then given of the main numerical techniques presently available for the coupling problem. The global state of the art and possible extensions are looked at through the viscous methods for airfoils. New results are presented for trailing-edge separation, and an approximate method is suggested to capture numerically the viscous interaction under the shock-waves.

COMPUTATION OF FLOWS INCLUDING STRONG VISCOUS INTERACTIONS WITH COUPLING METHODS

J.C. LeBalleur

I. INTRODUCTION

High Reynolds numbers flows are characterized by the existence of very rapidly changing localized phenomena that closely associate the effects of viscosity and turbulence, generally contained in the thin layers, and their effect on the structure of non-dissipative flows. A typical example of such a condition is the shock-boundary layer interaction. /1*

These concentrated and small-scale phenomena may condition the macroscopic flow completely, owing to the non-linearity of the equations which govern them and which generate complex flow conditions, called strong viscous interactions, in contrast to flows with weak interactions which are fundamentally different and lead to solutions close to conventional approximations of inviscid flows.

Notwithstanding the considerable progress made in adapting numerical methods to the resolution of complete Navier-Stokes equations, which in principle are able to process strong interacting flows, a purely mathematical approach to the aerodynamic problem remains difficult to the extent where it remains highly dependent upon the accuracy of the numerical techniques, the preparation of large enough turbulence models, the necessary recourse to very fine meshworks requiring the use of very power, and still unavailable, computer means.

Accordingly, a more physical approach is present in all practical numerical aerodynamics. It appears, among

*Numbers in the margin indicate pagination in the original text.

other places, when introducing equations for boundary conditions or for simplified local "models", when preparing composite resolution methods based on the coupling of several distinct numerical methods, when it is necessary to use meshworks adapted to local flow conditions. It is clear that the origin of such methods is intricately interrelated with the multiple-scale structure of the flow as well as with the existence of approximated equations and numerical methods adapted to each scale. The adaptation of these methods to the physics of the phenomena has often proven to be a source of efficiency, particularly for relatively modest levels of viscous approximation. A typical example is given by the difficult calculation of transonic airfoils for which methods based on inviscid flow and interacting boundary layer analyses exhibit even better performances than the Navier-Stokes type analyses, both in terms of computer costs and their accuracy.

On the long-term, we may conclude that the adaptation of coupling methods to the specific physical aspects of high Reynolds numbers should lead, in conjunction with the development of direct resolution methods, to greater economy for equal performances, or to the processing of more complex problems for a given computer cost (three-dimensional flows, for example), or to an indirect development of new numerical techniques for resolving Navier-Stokes equations. /2

Parts 2 and 3 of this report will succinctly examine the approximation levels and the general concepts which seem to be outlined from current methods of computing flows with strong viscous interactions. Parts 4, 5 will discuss methods based on simple viscous approximations, obtained from Prandtl or thin layer hypotheses. After discussing their effects on a computer model by coupling

with the inviscid flow, we will briefly survey the numerical methods currently capable of resolving a coupling of this type, which is a basic problem whose study is still very recent and limited. Finally, we will take a look at the capabilities and future prospects for the coupling methods of this category by examining an example offering a synthesis of transonic airfoils where various interacting viscous phenomena interfere.

2. NUMERICAL APPROXIMATION OF VISCOUS FLOWS: GENERAL LEVELS OF ANALYSIS AND COUPLING METHODS

It is not within the scope of this brief analysis to review the various methods used to calculate viscous flows, as our objective here is simply to offer a qualitative outline of the main approximation methods, the possible approximation levels, and their application limits.

As shown in figure 1, a classification into four levels seems conceivable; level I combining the various methods based on a direct resolution, while levels II, III, IV correspond to the main indirect approaches or coupling methods. Although relatively strong approximations may be used for each level, which prohibits a rigorous structural organization, the general nature of the most complete methods of each category increases from level IV to level I.

2.1. Methods of Direct Resolution

Level I corresponds to the methods of direct resolution and includes in particular the complete resolution of the Navier-Stokes equations, as well as the resolutions limited to large-scale turbulent structures, with modelization of fine structures. From a standpoint leaning toward methods currently usable in applications, level I corresponds to an

approach which may be qualified as a general approach [1 to 4] to the extent that it adopts the same numerical method and the same system of equations which are uniformly valid in the entire flow field. We are referring to averaged Navier-Stokes equations, associated with a turbulence model, or Navier-Stokes equations truncated by thin layer approximations [5,6].

2.2. Direct Methods With Equation Commutation

The first extension of the overall approach consists of retaining a single numerical method, but by commutating the resolved equations over the complete or simplified systems [7], figure 2, as a function of the calculation regions. This approach, similar in its intentions to the methods of coupling by regions, cannot be regarded identical to it. It is actually clear that the equation commutation boundaries thus employed do not in any way materialize distinct regions of numerical calculation, linked by their boundary conditions alone; on the contrary, a numerical continuity of the derivatives at the commutation boundaries is implicitly postulated. The approach of commuting equations by region essentially consists of simplifying the calculations by assuming a priori that part of the equation terms are discarded in certain regions, in accordance with the precision of the numerical resolution technique. This simplification may be completed by optimizing the geometry of the commutation boundaries.

2.3. Strong Coupling Methods With Division Into Computation Regions

The equation commutation approach may generate new mathematical or numerical problems compared to an overall approach with complete Navier-Stokes equations, in the event

of a large truncation of these. For example, they will be associated with order changes in equations with partial derivatives, changes in the domain of dependence and in the required boundary conditions.

This leads us to level II and to the coupling approach by separating the computation regions (figure 3) in which the mathematical and numerical problems are treated separately, while the overall problem is restored by means of a rigorous coupling, called strong coupling, between the boundary conditions of the various sub-regions along their common boundaries. The equations used in the various sub-regions are generally either complete Navier-Stokes equations, or Prandtl or Euler equations truncated in thin layer approximations [8, 9, 10, 11].

Changes in the order and nature of equations with partial derivatives with computation sub-regions forces us to modulate the number of coupling conditions along the common or connecting boundaries, and to make selections on the basis of the physics of the phenomena as well as on the nature of the local equations. The coupling of aerodynamic parameters to a connecting boundary no longer leads in this particular case to a linking of their normal derivatives to this boundary, the lack of residual connection being representative of the precision of the coupling model, for a determined division of regions and equations.

Note that the transition from level I to level II creates a new numerical problem. This consists of making a strong coupling of boundary layers associated with various sub-problems, using iterative or implicit methods in steady or unsteady conditions. It is clear that this major problem could not be summarized by establishing a computation flow chart, and in aerodynamics it has been the subject matter of a limited number of studies essentially motivated

by linking the Euler and Prandtl equations (see paragraph 5).

/3

2.4. Methods Of Strong Coupling With Division Into A System Of Equations

The technique described above of the division into domains supposes that in each of them the equations resolved themselves describe the local behavior of the flow. In the case of modest approximation levels, like that of the Prandtl equations, such a condition may lead to large limitations. It should be remarked that such a connecting technique is to be avoided in the analytical methods of connected asymptotic expansions, in which the calculation domains associated with the various scales become superposed in the same physical domain.

We have found [3, 12 to 15] that the introduction of overlapping calculation domains, (figure 4) in the formulation of coupled composite methods for calculating viscous flows at high Reynolds number, could lead to considerable progress, physically related to the possibility of processing the viscous flow in terms of differences with the fictive inviscid flow which it is the closest to. This analysis constitutes a generalization of the boundary layer methods, whether conventional or with strong coupling along a wall, which we will assume to be plane in order to simplify the presentation, if \bar{u} and \bar{v} are the components for the velocity, $\bar{\rho}$ the density and \bar{p} the pressure, if u, v, ρ, p are their homologues for the overlaid inviscid flow, the equations for the viscous flow, notated ① + ② will be dissociated into a system of inviscid flow equations, notated ① and into a system of matching viscous equations notated ②. The unsteady dynamic equations therefore become:

$$(1) \quad \left\{ \begin{array}{l} \frac{\partial \rho u}{\partial x} + \frac{\partial \rho v}{\partial y} = 0 \\ \frac{\partial \rho u^2}{\partial x} + \frac{\partial \rho uv}{\partial y} = - \frac{\partial p}{\partial x} \\ \frac{\partial \rho uv}{\partial x} + \frac{\partial \rho v^2}{\partial y} = - \frac{\partial p}{\partial y} \end{array} \right. \quad (2.1)$$

$$(2) \quad \left\{ \begin{array}{l} \frac{\partial \rho u - \bar{\rho} \bar{u}}{\partial x} + \frac{\partial \rho v - \bar{\rho} \bar{v}}{\partial y} = 0 \\ \frac{\partial \rho u^2 - \bar{\rho} \bar{u}^2}{\partial x} + \frac{\partial \rho uv - \bar{\rho} \bar{u} \bar{v}}{\partial y} = - \frac{\partial p - \bar{p}}{\partial x} - \frac{\partial \sigma_x}{\partial x} - \frac{\partial \tau_{xy}}{\partial y} \\ \frac{\partial \rho uv - \bar{\rho} \bar{u} \bar{v}}{\partial x} + \frac{\partial \rho v^2 - \bar{\rho} \bar{v}^2}{\partial y} = - \frac{\partial p - \bar{p}}{\partial y} - \frac{\partial \sigma_y}{\partial y} - \frac{\partial \tau_{xy}}{\partial x} \end{array} \right. \quad (2.2)$$

$\sigma_x, \sigma_y, \tau_{xy}$ represent the stress tensor components. This matching formulation of the viscous problem leads to a very similar resolution as in the method of coupling by domains, owing to the strong coupling that must be achieved between and the boundary conditions so that:

$$0 = \lim_{y \rightarrow \infty} [f - \bar{f}] \quad \text{with } f = \{u, v, p, \rho\} \quad (2.3)$$

We may still notice that the importance of selecting the external boundary of the viscous layers $y = \delta(\hat{x})$, which is relatively arbitrary in the method of coupling by linking the domains, is eliminated.

An advantage of the matching formulation (2.2) appears clearly by approximating with intermediary assumptions which fall between Prandtl's assumptions and those of Navier-Stokes equations for thin layers. We therefore have:

$$\left\{ \begin{array}{l} \frac{\partial \rho u - \bar{\rho} \bar{u}}{\partial x} + \frac{\partial \rho v - \bar{\rho} \bar{v}}{\partial y} = 0 \\ \frac{\partial \rho u^2 - \bar{\rho} \bar{u}^2}{\partial x} + \frac{\partial \rho uv - \bar{\rho} \bar{u} \bar{v}}{\partial y} = - \frac{\partial \tau_{xy}}{\partial y} \\ \frac{\partial \bar{p} - \bar{p}}{\partial y} = 0 \end{array} \right. \quad (2.4)$$

which, according to (2.3), gives $\bar{p}(x, y) = p(x, y)$.

This approximation of the pressure is much less restrictive than that deduced from the Prandtl equations in a coupling by linking the domains:

$$\frac{\partial \bar{p}}{\partial y} = 0 \quad \bar{p}(x, y) = \bar{p}(x) = p(x, \delta) \quad (2.5)$$

while the resolution of the parabolic system (2.4) with u, v, p, \bar{p} , given by (2.1) is as complex as the resolution of simple Prandtl equations.

In the event of less extensive simplifications than (2.4), or of an application of the Navier-Stokes equations (2.2), the selection of the matching formulation becomes intricately related to the selection and conditioning of the numerical techniques applied to (2.1) and (2.2) as well as to their coupling. Finally, we will note that at approximation level II in figure 1, the division made into a system of viscous and non-viscous equations implies an analysis of a strong interacting coupling, which corresponds to a strict resolution of (2.1) (2.2) (2.3), and which accounts for the influence exerted by the downstream flow on the upstream flow. Approximations of this type, although relatively simplified, have been studied recently [16, 17, 18]. Conversely, other approaches maintain approximations of systems of parabolic equations, resolved directly from upstream to downstream, which makes them

comparable to boundary layer methods for weak interactions of level IV [19, 20].

2.5. Weak Coupling Methods

Approximation levels I and II correspond to a modelization of the viscous flow capable of describing flows of strong viscous interactions, at least qualitatively, owing to the viscous equations resolved or to the strong coupling effect at the inviscid flow, in the case of the simplest viscous equations. We should still consider that this capacity of processing regions of strong interaction implies the use of suitably fine interconnections in order to be effective, for any equation resolved. In turbulent flows, even for the simplest systems of equations, the resolution scales should not be coarser than the local thickness of the viscous layers involved.

Levels III and IV correspond to simplified analyses whose application generality is smaller, but which remains the support of most current applications. The most commonly used are the boundary layer methods of level IV, used in conjunction with conventional inviscid flow calculations, resolved in uncoupled mode. The absence of a coupled resolution comes from the concept of a weak interaction or coupling, related to the asymptotic second order theory of the boundary layer in laminar cases [21], and to theories of the same nature in turbulent cases [22,23].

Figure 5 shows the scheme of the simplification made at the coupling level. In a first approximation, the field of inviscid flows is obtained independently of any boundary layer. It determines a simplified pressure field for the boundary layer which makes it possible to calculate the boundary layer and its displacement thickness in the

first approximation. This makes it possible to determine the final approximation of the inviscid flow, as well as that of the boundary layer pressure field. A second order approximation may then be calculated for the boundary layer, which then always has a normal predetermined pressure gradient, but which is not zero in the case of a wall camber. The coupling is "weak" provided that the viscous layer is completely conditioned for a given approximation order by the inviscid flow upon which no mutual influence is exerted.

In this analysis, the notion of iteration on the viscous displacement thickness is absent and is replaced by a direct and single correction. Any shortcoming in such a single correction precisely marks the appearance of phenomena of strong viscous interactions, related to the separations, shock waves, trailing edge, as well as to the necessity for multiple layered models if we still want to use asymptotic theories [23 to 31] without being able to eliminate the appearance of a strong coupling problem.

A characteristic property of a weak asymptotic coupling is that it leads to the resolution of a parabolic system, for the viscous problem, in which we do not know the effect exerted by the downstream flow on the upstream flow. Such an influence can be determined only through the boundary conditions set by the inviscid flow, and which is therefore totally eliminated for a supersonic external flow, or even in the approximation of a one-dimensional subsonic inviscid flow.

The corresponding simplification made of the resolution can therefore be carried out upstream to downstream, and has been the subject of transpositions in methods abandoning the simple Prandtl equations for less restrictive equations, qualified at level Iv in figure 1 of the

parabolic approximations of the Navier-Stokes equations. In this case, the Navier-Stokes equations were first subjected to thin layer approximations, which consisted of eliminating the viscous diffusion terms according to Ox , if Ox represents the direction of the main flow. This simplification of levels I or II is not self-sufficient in the general case where the system of equations is completely parabolized in the direction of positive x 's, particularly in the presence of subsonic flow regions [32, 33]. We may therefore speak of systems of elliptical equations because of the pressure field, provided that the systems remain parabolic either when the pressure is fixed, or when its mean longitudinal variation along x is fixed, while its secondary variation in plane yOz is calculated [34], or when the longitudinal pressure variation is also calculated upstream to downstream, but at the cost of a quasi-one-dimensional approximation and of a pressure change in the momentum equation according to Ox [35].

In all of the cases, the switch from such a parabolized weak coupling problem to an elliptical strong coupling problem of level I or II, implies the addition of an iteration on the pressure, capable of eliminating at convergence the various approximations used for each parabolized iteration [16, 17, 34, 36].

2.6. Intermediary Methods Between Weak And Strong Couplings /5

Figure 1, of level III, shows examples of this type of analysis. The first may be given through an progressive extension of the methods of computing airfoils. Starting with the obvious short-coming of a weak coupling approach, an extension toward the investigation of a strong coupling was progressively developed, by means of iterations on the viscous displacement effect. Although the approximation levels obtained differed considerably between the different

methods, for example [15, 29, 37 to 40], either because of the use of smoothings or relatively arbitrary modelizations of the displacement thickness, or due to numerically or analytically incomplete coupling techniques in regard to separations, trailing edges, boundary layer/shock wave interactions or calculation meshings, it is clear that the overall variation should lead to strong coupling methods of level II.

A second category of intermediary methods between weak and strong couplings is given by forming a model of inviscid flow separations. A first example is given here by calculating inviscid flows containing vortex sheets issuing from predetermined separation lines [41]. A second example is that of forming models of large separations by calculating free isobar boundaries in an inviscid flow. These models are especially used in stall problems [42].

3. BOUNDARY CONDITIONS OF INVISCID FLOWS - DISPLACEMENT

The methods of calculating inviscid flows is based on the slip condition expressing wall tightness, and on the Joukowski condition which when used seems to recall alone that the objective is to form a model of a viscous flow. The calculation also brings to light, in regard to weak solutions, the slip sheets through which the normal velocity and pressure are continuous.

If the physical problem is approached by analyzing a viscous flow, at the scale of a continuous medium, such slip conditions become impossible for any Reynolds number and it is the asymptotic theory of the boundary layer which tells us that the external non-viscous flow to be considered is subjected to these slip conditions, in a first approximation. These slip conditions therefore acquire an origin related to the viscosity. At the

second approximation order, a normal non-zero velocity on the walls, as well as a normal velocity and pressure discontinuity on the slip sheets, express the viscous displacement effect on the residual inviscid flow region. If indices 1 and 2 designate the successive orders of approximation, we have for example:

$$\left. \begin{aligned} y &= \mathcal{R}^{-\frac{1}{2}} \bar{y} & \mathcal{R} &= \text{Reynolds} \\ \delta_1^*(x) [\rho_1 u_1]_{(x,0)} &= \mathcal{R}^{-\frac{1}{2}} \int_0^{\infty} \left\{ [\rho_1 u_1]_{(x,0)} - [\bar{\rho}_1 \bar{u}_1]_{(x,\bar{y})} \right\} d\bar{y} \\ [\rho_2 v_2]_{(x,0)} &= \frac{d}{dx} [\rho_1 u_1 \delta_1^*]_{(x,0)} \end{aligned} \right\} \quad (3.1)$$

3.1. Strong Coupling Along Adjoining Regions

The transposition of these conditions to coupling problems at finite Reynolds number was initiated by Crocco and Lees [43] to calculate supersonic separations in a strong coupling approach along adjoining regions (figure 6) using the Prandtl equations for $0 < y < \delta(x)$, δ being the physical thickness of the boundary layer. In the most usual case where only one boundary condition of viscous origin in $y = \delta(x)$ is needed for determining the inviscid flow, the relationship used by Crocco and Lees is general, since it is based only on the integration of only one equation of continuity in y . If $K(x)$ is the wall camber:

$$\left. \begin{aligned} \left[\frac{v}{u} \right]_{(x, \delta)} &= \frac{1}{1 + K\delta} \left\{ \frac{d\delta^*}{dx} - (\delta - \delta^*) \left[\frac{1}{\rho u} \frac{d\rho u}{dx} \right]_{(x, \delta)} \right\} \\ \delta^*(x) [\rho u]_{(x, \delta)} &= \int_0^\delta \left\{ [\rho u]_{(x, \delta)} - [\bar{\rho} \bar{u}]_{(x, y)} \right\} dy \end{aligned} \right\} \quad (3.2)$$

This displacement formulation $\delta^*(x)$ is exempt from approximation other than that associated with the calculation of $[\bar{\rho} \bar{u}] (x, y)$.

Other methods of introducing the coupling condition (3.2) in the calculation of inviscid flows are frequently used. It may seem more convenient to consider that there is either no flow through the boundary of the inviscid flow, and we are then speaking of a displacement concept, or that this boundary is simply based on the wall. In the two cases, a certain equivalence with (3.2) may be obtained by considering an approximated analytical shift of (3.2) from $y = \delta(x)$ in $y = \gamma(x)$. The equation of non-viscous continuity gives:

$$\left[\frac{v}{u} \right]_{(x, \gamma)} = \left[\frac{v}{u} \right]_{(x, \delta)} - (\gamma - \delta) \left[\frac{1}{\rho u} \frac{d\rho u}{dx} \right]_{(x, \gamma)} + \dots \quad (3.3)$$

which leads to a slip condition if $\gamma = \delta^*$, an injection condition if $\gamma = 0$ and if the corresponding expressions for $\delta^*(x)$:

/6

$$\left[\frac{v}{u} \right]_{(x, \delta^*)} = \frac{d\delta^*}{dx} + \dots \quad (3.4)$$

$$[\rho v]_{(x, 0)} = \frac{d}{dx} [\rho u \delta^*]_{(x, 0)} + \dots \quad (3.5)$$

$$\delta^*(x) [\rho u]_{(x, \gamma)} = \int_0^\delta \left\{ [\rho u]_{(x, \gamma)} - [\bar{\rho} \bar{u}]_{(x, y)} \right\} dy \quad (3.6)$$

The displacement formulations (3.4) (3.5) (3.6) are still approached, as well as the equivalence with (3.2). The

asymptotic validity of this equivalence when $\eta \rightarrow \infty$ is not automatic where the expansion order (3.3) depends on the order of $d\rho\mu/dx$, a quantity often not bound when in the asymptotic theories with multiple layers. The formulations (3.4) (3.5) may still be outlined from any approximation by selecting new definitions for $\delta^*(x)$.

3.2. Strong Coupling Along Overlapping Regions

Such a change in the definition of $\delta^*(x)$ is easily done by introducing (figure 7) overlapping calculation regions over which the viscous equations are segmented as described in paragraph 2.4. In this case, the simple integration of the continuity equation (2.2) in y gives, since

$$\left. \begin{aligned} 0 &= \lim_{y \rightarrow \infty} [\rho v - \bar{\rho} \bar{v}] : \\ &[\rho v]_{(x,0)} = \frac{d}{dx} [\rho \mu \delta^*]_{(x,0)} \\ &\delta^*_{(x)} [\rho \mu]_{(x,0)} = \int_0^\infty \{ [\rho \mu]_{(x,y)} - [\bar{\rho} \bar{\mu}]_{(x,y)} \} dy \end{aligned} \right\} \quad (3.7)$$

This generalization of the definition of $\delta(x)$ takes into account the normal pressure gradients inside the viscous layer, through variations in y of the viscous term $\bar{\rho} \bar{\mu}$ and of the non-viscous term $\rho \mu$; these may possibly be rapid, even discontinuous, unlike boundary layer analyses. A schematic illustration is given in figure 8, for the case where $(\bar{\mu}/\mu) = \phi(x, y)$ is assumed to be a continuous function.

A formulation of $\delta^*(x)$ adapted to the displacement concept may likewise be defined:

$$\left. \begin{aligned} \left[\frac{\sigma}{\mu} \right]_{(x, \delta^n)} &= \frac{1}{1 + K\delta^n} \frac{d\delta^n}{dx} \\ \int_{\delta^n}^{\infty} [\rho\mu]_{(x,y)} dy &= \int_0^{\infty} [\bar{\rho}\bar{\mu}]_{(x,y)} dy \end{aligned} \right\} \quad (3.8)$$

All things considered, use of a displacement thickness to formulate a coupling problem is in no way the same as using boundary layer approximations.

4. SIMPLE APPROXIMATIONS OF THE VISCOUS FLOW - INFLUENCE OF A STRONG COUPLING

For both historical and practical reasons, current coupling methods have been mainly developed on the basis of boundary layer assumptions. We will confine ourselves in the remainder of this report to this class of methods, using either Prandtl equations, or a similar extension of thin layer equations, described in paragraph 2.4, in which the pressure $\bar{p}(x, y)$ is identified with that of the non-viscous calculation $p(x, y)$.

4.1. Separation and Reverse Flow Regions

The boundary layer problem, subjected to the Prandtl equations and decoupled from the inviscid flow, must be formed by an external boundary layer condition, for which the pressure $p(x, \delta)$ has been used for a long time in the same way as in the asymptotic theories of weak interactions. We thus know the singular behavior of Goldstein [44] for "square roots" offered by solutions near a position of zero friction in two-dimensional steady flows, a behavior also offered by integral boundary layer methods [12]. In unsteady flows [45] or three-dimensional flows [46], the integral methods demonstrate a different type of singularities which are formed of discontinuities of integral

thicknesses associated with the weak solutions of equation systems, which are no longer initially localized in reverse flow regions, and which might explain certain numerical anomalies found in the solution of the Prandtl unsteady equations with reverse flows and a set pressure field.

However, we were able to show that these singular behaviors should not be confused with a validity limit of the Prandtl equations, or with an abrupt separation from the viscous layer and from the wall, but that they result from the pressure selected for the external boundary condition. When the pressure becomes a calculation unknown, either by formulating an inverse problem subjected to an external condition, or by coupling with the inviscid flow, consistent and realistic solutions were obtained for small separations [12, 47 to 55]. The same behavior was observed for unsteady conditions [45]. Yet it is still clear that the Prandtl problem for strong couplings with the external inviscid flow no longer constitutes a parabolic system free of downstream effects, even without the reverse flows, owing to the boundary condition, unknown a priori, formed by the external pressure distribution with coupling effect (figure 6).

4.2. Downstream Influence On The Upstream In Supersonic And Transonic Flows

The essential question raised by the matching calculation of the Prandtl and Euler equations is the following: is the elliptical nature of the unsteady Navier-Stokes equations also found in the coupling model when the inviscid flow is locally supersonic so that the downstream influence on the upstream cannot have an exclusively non-viscous origin? Since Crocco-Lées' first work, a

/7

a long investigation was conducted [12, 14, 56 to 59] and the answer found was positive for "subcritical" viscous layers, and negative for "supercritical layers."

In the subcritical case, the coupling of hyperbolic non-viscous equations with parabolic viscous equations leads to a problem of initial conditions which is improperly presented, to the extent where an exponential amplification of any initial disturbance occurs on a short scale, corresponding to the boundary layer thickness, approximately, according to a branching solutions process. The aspect of an improperly presented problem is eliminated if one of the boundary conditions is transferred from upstream to downstream, which reveals the elliptical nature of the model. Furthermore, the branching process generally makes it possible to introduce such a downstream boundary condition as a purely optional constraint which is the case in the coupling model for the boundary conditions currently applied to the downstream in Navier-Stokes type calculations. The occurrence of a downstream to upstream influence due to the coupling effect also finds a theoretical support in strong interaction asymptotic theories, such as the triple-deck laminar model, for example. We were also able to verify numerically that the supersonic triple-deck equations are also asymptotic solutions of the coupling model, when the Reynolds number moves toward infinity [27], figure 9.

In the supercritical case, the elliptical nature of the viscous equations is only partially found in Chocco-Lees coupling model, by means of weak solutions whose pressure jumps suddenly transform the supercritical layers into subcritical layers, each time a downstream influence on the upstream is locally indispensable. The supercritical behavior is therefore found agains near the downstream after passing a "critical point," where

the stability required of the solution plays the role of a supplementary downstream condition for the subcritical region [59]. A simple interpretation of the behavior patterns of the model in the vicinity of jumps and critical points may be directly deduced from the local behavioral patterns of the branching solutions, as well as the stabilizing boundary conditions needed, see figures 10 to 11.

The preceding gaps in the Crocco-Lees model are not related to the approximations used to solve the Prandtl equations if an integral method is used, as was often believed to be the case, but are actually due to the simplified pressure field $\bar{p}(x) = \bar{p}(x, \delta)$ of the viscous layer. In an integral method the relationship (3.2) leads to a quasi-linear relationship between the viscous deflection $\theta = (\eta/\mu)$ and the pressure gradient in $y = \delta(x)$:

$$D_1 \theta = D_2 \delta^* \frac{dp}{dx} + D_3 \quad (4.1)$$

D_1 vanishes to zero for separations or for reattachments where the pressure gradient cannot be any value, but must be $\delta^*(dp/dx) = -(C_3/D_2)$ to assure the regularity of the solutions. D_2 reduces to zero at the critical points, where the regularity forces $\theta = (D_3/D_1)$. The symmetry of the Goldstein and Crocco-Lees singularities may be noted for the coupling model for adjoining regions. The relationship (4.1) or simply

$$\theta = B \frac{dp}{dx} + C, \quad B = \frac{D_2}{D_1} \delta^* \quad (4.2)$$

is a determinant for the branching solutions, which are stable according to x if $B < 0$, and unstable if $B > 0$. For an attached layer, the unstable case corresponds to a subcritical behavior and to an elliptical type problem. Note, however, that in the case of a separation, D_1 changes its sign, and therefore so does B , and this leads to table branching solutions in the separated region and the downstream effect on the upstream has the

result of selecting stable solutions at the reattachment point, figure 12. In the case of a local solution of the Prandtl equations, we are left [57] with a relationship analogous with (4.2), demonstrating the importance of the local Mach number \bar{M} in supercritical behaviors:

$$B = \lim_{\epsilon \rightarrow 0} \int_{\epsilon}^{\delta} \frac{1 - \bar{M}^2}{\delta \bar{M}^2} dy \quad (4.3)$$

The limit $\epsilon \rightarrow 0$, often being singular, the behavior of the branching solutions is generally not deduced directly from (4.3), see [3, 12, 15]. Nevertheless, it follows from (4.3) that the supercritical behaviors ($B < 0$) can be derived only from the presence of supersonic viscous regions, and that they are highly dependent upon the selection of the boundary δ in the matching model. Any subcritical coupling may thus be converted into a supercritical coupling, by selecting a boundary $y = \delta(x)$ farther away from the wall [3].

The subcritical or supercritical nature of Crocco-Lees therefore is not an intrinsic property of the viscous layer, but of the adjoining coupling model [3, 15]. Its physical interpretation should therefore call on the external inviscid flow. We may thus note that the supercritical behavior of a supersonic separation at increasing Mach number appears only when the focalization shock wave approaches until it reaches the external boundary of the viscous layer, with any penetration inside the viscous layer being excluded by the calculation model and being simulated by a pressure jump, figure 13.

/8

4.3. Approximated Treatment Of the Normal Pressure Gradient. Matching Formulation

The shortcomings just described of the simple Crocco-Lees model for processing flows with strong viscous interaction in supersonic states, as well as in transonic states ($M \pm 1.20$), are the result of a too simplified pressure field $\bar{p}(x) = p(x, \delta)$. However, we have found [3, 12, 13, 15] that it is quite easy to discard these shortcomings by establishing a matching formulation of the viscous calculation, corresponding to the viscous calculation regions and the overlapping non-viscous regions, figure 7, as described in paragraph 2.4., and if the approximation over the pressure becomes $\bar{p}(x, y) = p(x, y)$.

By retaining only Prandtl's viscous term in the system (2.2), we obtain by integrating in y the equation of motion along x and its first moment relative to u :

$$\frac{\partial}{\partial x} \left\{ \int_0^\infty [\rho u^2 - \bar{p} \bar{u}^2]_{(x, y)} dy \right\} - [\rho u v]_{(x, 0)} = \tau_{(x, 0)} - \frac{\partial}{\partial x} \int_0^\infty [\bar{p} - \bar{p}]_{(x, y)} dy \quad (4.4)$$

$$\frac{\partial}{\partial x} \left\{ \int_0^\infty [\rho u^3 - \bar{p} \bar{u}^3]_{(x, y)} dy \right\} - [\rho u^2 v]_{(x, 0)} = \rho u^3 \phi - 2 \int_0^\infty \frac{\partial \bar{p}}{\partial x} [\bar{u} - \bar{u}] dy + 2 \int_0^\infty \bar{u} \frac{\partial \bar{p} - \bar{p}}{\partial x} dy \quad (4.5)$$

while the equation of motion in $[x, \delta(x)]$ gives the entrainment equation:

$$\text{with } \left\{ \begin{array}{l} \frac{d\delta}{dx} - \left[\frac{\rho v}{\rho u} \right]_{(x, \delta)} = E \\ \phi = \frac{2}{[\rho u^3]_{(x, 0)}} \int_0^\infty \tau \frac{\partial \bar{u}}{\partial y} dy \end{array} \right. \quad E = \left\{ \frac{\partial \tau / \partial y}{\rho u [\partial(u \cdot \bar{u}) / \partial y]} \right\}_{(x, \delta)} \quad (4.6)$$

The approximation $\bar{p}(x, y) = p(x, y)$ also discards the last term in (4.4) and in (4.5). If we define the generalized integral thicknesses for motion and kinetic energy in an analogous mode to that adopted for the displacement thickness in (3.7):

$$\left. \begin{aligned}
[\delta^*(x) + \theta(x)] [\rho u^2]_{(x,0)} &= \int_0^\infty [\rho u^2 - \bar{\rho} \bar{u}^2]_{(x,y)} dy \\
[\delta^*(x) + \theta^*(x)] [\rho u^3]_{(x,0)} &= \int_0^\infty [\rho u^3 - \bar{\rho} \bar{u}^3]_{(x,y)} dy \\
\delta_i^*(x) u_{(x,0)} &= \int_0^\infty [\mu - \bar{\mu}]_{(x,y)} dy
\end{aligned} \right\} \quad (4.7)$$

We obtain integral equations very close to those derived with the Prandtl equations:

$$\left[\frac{d\theta}{dx} + \frac{\delta^* + 2\theta}{u} \frac{\partial u}{\partial x} + \frac{\theta}{\rho} \frac{\partial \rho}{\partial x} \right]_{(x,0)} = \frac{Cf}{2} \quad (4.8)$$

$$\left[\frac{d\theta^*}{dx} + \frac{\theta^*}{\rho u^2} \frac{\partial \rho u^2}{\partial x} + 2 \frac{\delta^* - \delta_i^*}{u} \frac{\partial u}{\partial x} \right]_{(x,0)} = \phi + \phi_p \quad (4.9)$$

Note, however, that the kinetic energy equation (4.9) requires a modelization of a term for the normal pressure gradient ϕp , related to the variation of $\partial p / \partial x$ in y in (4.5), whereas the entrainment equation (4.6) does not require it. A certain approximation is still present, however, if the entrainment equation (4.6) is transformed so that only the following terms occur: $\rho(x,0)$, $u(x,0)$, $v(x,0)$:

$$\left[\frac{d\delta}{dx} - \frac{d\delta^*}{dx} + \frac{\delta - \delta^*}{\rho u} \frac{\partial \rho u}{\partial x} \right]_{(x,0)} = E \quad (4.10)$$

Besides the benefit of accounting for an approximated normal pressure gradient, the matching formulation (3.7) (4.7 to 4.10) leads us to replace the integral B in (4.3) with an integral B' [12] for the analysis of supercritical behaviors:

$$\left. \begin{aligned}
B' &= \lim_{\epsilon \rightarrow 0} \int_{\epsilon}^{\infty} \frac{M^2 - \bar{M}^2}{\gamma \rho M^2 \bar{M}^2} dy \\
M(y) &= \text{nonviscous} \\
\bar{M}(y) &= \text{viscous}
\end{aligned} \right\} \quad (4.11)$$

The first improvement, common to (3.7) (4.7 to 4.11)

is to totally discard the relatively arbitrary role of the adjoining boundary $y = \delta(x)$. Secondly, the term $(1 - \bar{M}^2)$ in (4.3), generator of supercritical behaviors when $\bar{M} > 1$, is replaced by $(M^2 - \bar{M}^2)$, a term which is most likely always positive. We were thus able to conclude [12] that the coupling along overlapping regions always leads to subcritical behaviors, where the downstream influence on the upstream is fully observed, and where the pressure distributions on the walls $p(x, 0)$ are always continuous. Consequently, the possible shock waves always generate by focalization within the non-viscous calculation region, which may even occur within the viscous layers, figure 14. In these intense cases of normal pressure gradient, a second order may be applied a posteriori to the approximation $\bar{p}(x, y) = p(x, y)$, in the form:

/9

$$\left[\frac{\partial p - \bar{p}}{\partial y} + K(x) [e u^2 - \bar{p} \bar{x}^2] \right] (x, y) \quad (4.12)$$

$K(x)$ is a mean camber of the streamlines, which may be indistinguishable from that of the walls or mean lines of waves only in regions of weak interactions. At the wall, or at the center of a wake, we obtain:

$$p(x, 0) - \bar{p}(x, 0) = K(x) [\delta^*(x) = \theta(x)] \quad (4.13)$$

Finally, it should be pointed out that the supercritical behaviors, eliminated in the preceding overlapping coupling should still be possible in the coupling by adding a displacement thickness, where relationship (4.11) becomes:

$$B^* = \lim_{\epsilon \rightarrow 0} \left[\int_{\epsilon}^{\delta^*} \frac{1 - \bar{M}^2}{\gamma \bar{p} \bar{M}^2} dy \right] + \int_{\delta^*}^{\infty} \frac{M^2 - \bar{M}^2}{\gamma \bar{p} M^2 \bar{M}^2} dy \quad (4.14)$$

an integral in which the first term may always be negative,

threshold of transition to supercritical behavior therefore being essentially $M = 2$ for a flat plate turbulent layer.

5. NUMERICAL METHODS FOR STRONG COUPLINGS

The simplifications brought to the resolution of the viscous fluid, at level II in figure 1, by segmentation of the calculation regions or of the equations used, have another role of artificially generating a strong coupling numerical problem. In the case of a coupling by adjoining regions, it is necessary to assure a rigorous compatibility of the boundary conditions of the various sub-problems on their common boundaries. Since the nonlinearity of the viscous equations in practice makes an iterative solution inevitable, it may be assumed that the problem remains virtually the same in the coupling by segmentation of the equations, with overlapping calculation regions.

5.1. Nature Of The Problem

This strong coupling of the boundary conditions over the interfaces of the various constituent calculations requires a less rigorous numerical resolution than that used in each subproblem, with the risk of degenerating the strong coupling treatment into a weak coupling approximation. This condition is reinforced by the high sensitivity of the inviscid flow calculations to the accuracy of the numerical treatment of the boundary conditions. It is even more sensitive if we consider that in thin layer viscous problems, the coupling effect alone can change the mathematical nature of the behavior of the various subproblems, via branching solutions reviewed in paragraph 4.2 and lead to differences of about 1 between the solutions subjected to a rigorous coupling and those derived

with an approximated coupling.

If the finite differences methods are used, for example, the coupling must be made in each discretization node of the interface with the consistent numerical schemes, compatible to those used in each region. The interpolation over the interface is conceivable in the case of discontinuous meshes, provided that it is consistent with the numerical scheme order, and with the regions of mathematical influence. Conversely, the use of smoothings or filtering is to be discarded, unless the technique may be reduced to the insertion of a numerical dissipation, which is evanescent when the discretization step leads to zero.

If we consider the solution of evolving problems, the same problem with a strong coupling may be overcome at each time step to avoid a viscous resolution inconsistent in time or a weak interaction approach. In the case of iterative relaxation or pseudo-unsteady methods, in which only the final solution matters, the stability in time may be disregarded. Conversely, coupling errors at each iteration should not augment and a specific stability study should be considered. The specificity and difficulty of such a study is due to the fact that although it is necessary to analyze the magnitudes bordering over the coupling interface, error increases is managed by an operator calling on the resolution of the subproblems adjacent to this interface, which defines a mathematical problem over a space whose dimension is larger than that of the interface where the coupling errors are studied.

Yet, it is clear that, apart from unusual circumstances, the definition of an iterative coupling method may be reduced to a simple definition of a calculation flow chart,

in the case of a strong coupling. In the first place, it is necessary for the coupling to select consistent numerical schemes, at least in terms of space, observing not only the dependency domains of the equations of each subregion calculated separately, but also the real dependency domain of the coupled mathematical problem, specifically accounting for the possible branching solutions. For example, the consistency will not be obtained for the coupling of the Euler and Prandtl equations along a locally supersonic boundary, with attached boundary layer, if the schemes with differences totally decentered upstream are used and if, at least for quantifying the coupling relationships, one of them does not escape this choice. On the contrary, we have shown in this case, the advantage of a decentering toward downstream [13].

In the second place, the generality of an iterative coupling method implies that the complex stability problem is mastered, for the purpose of adapting the relaxation techniques, i.e. modulating the stabilizing relaxation coefficients as a function of time intervals and local spaces, as well as of the aerodynamic magnitudes. This constraint is similar, to the necessity of calculating, in an explicit unsteady numerical method, the local maximum time interval compatible with the stability of the calculation as a function of the local space interval. /10

The elimination of this constraint has for a long time led to unstable iterations for boundary layer calculations over airfoils and to a relatively arbitrary use of smoothing techniques. These instabilities, which are purely numerical, are influenced by the weak or strong aspect of the local viscous coupling interaction, but they are not always absent if the discretization interval is small enough. They particularly appear for flat plate boundary

layers [60]. Figure 15 gives an illustration relative to the inviscid flow - unsteady boundary layer coupling [61] near a uniform flow over a flat plate. It shows that, all other things being equal, a slight reduction in the space interval or increase in the time interval is sufficient for switching from a stable coupling iteration to an unstable iteration.

Finally, a reduction of the numerical instabilities of explicit type simple iterative coupling techniques, may obviously be investigated in the development of methods which process the coupling in a more implicit manner, for each iteration, or based on more general nonlinear numerical techniques.

5.2. Behavioral Law of The Steady Boundary Layer

Most of the viscous - nonviscous numerical coupling methods have a slightly implicit nature, for reasons of simplicity, application generality and interchangeability of the viscous and nonviscous modules. Recourse to viscous modules using Navier-Stokes equations, which are complete or in the approximation of thin layers, remains rare in the coupling methods [8 to 11, 32 to 34] for the part specific to the coupling. Conversely, more accurate methods are outlined in the case of simple viscous approximations as described in paragraph 4.

In the case of integral boundary layer methods, the problem to solve is essentially that of an inviscid flow whose boundary conditions are no longer known in advance. On the contrary, these become solutions of a system of ordinary differential equations on the boundary as, for example (3.7) (4.8) (4.9), relating the pressure $p(x,0)$, the angular direction of the flow $\theta(x,0)$ as well as the

viscous thicknesses. After a few eliminations, we may extract the relationship between $\theta(x,0)$ and $p(x,0)$ actually applied to the inviscid flow:

$$A_1 \theta = A_2 \delta^* \frac{dp}{dx} + A_3 \quad (5.1)$$

x is measured along the boundary of the inviscid flow - A_1, A_2, A_3, δ^* depend on other differential equations, on the initial values of the viscous thicknesses as well as on nonviscous variations $\theta(x)$ and $p(x)$. Equation (5.1) leads to highly nonlinear behaviors; A_1 is reduced to zero during separations or reattachments, A_2 is reduced to zero at the critical points when these were not eliminated. The small scale term δ^* leads to phenomena of branching solutions, whose importance was reviewed and which lead to the inclusion of supplementary downstream boundary conditions.

In the case where the integral boundary layer methods are replaced by local Prandtl viscous equations, the behavior of the viscous boundary, as a boundary condition of the inviscid flow, remains appreciably the same as (5.1), at least if we confine ourselves to an analysis of disturbances around a solution

$$\left[\theta_0(x,0), p_0(x,0) \right] : \quad A_1 [\theta - \theta_0] = A_2 \delta^* \left[\frac{dp}{dx} - \frac{dp_0}{dx} \right] \quad (5.1')$$

a relationship to compare with (4.2) (4.3) (4.11) (4.14). Use of the fundamental relationship (5.1) as a closing boundary condition of an inviscid flow calculation therefore represents in a schematic form the coupling problem to be solved, in the case of thin viscous layers. Note that the viscous relationship (5.1) does not give the variables $\theta(x,0)$ and $p(x,0)$ a symmetrical role; only the pressure has a function in the form of a derivative. This

major difference with the nonviscous problem undoubtedly is due to the thin layer aspect more than to the viscous approximations used.

5.3. Methods Of Initial Supersonic Conditions

The local function of relationship (5.1) initially led to an investigation of supersonic solutions to the strong coupling problem. In this case, the apparent simplification of the initial conditions methods, proceeding from upstream to downstream with simultaneous resolution of (5.1) was widely used by Crocco-Lees and numerous successors [32, 33, 43, 59, 62 to 66] particularly in the case of a simple wave. However, we know that the unstable branching solutions result in an incorrectly defined problem, requiring a technique of resolution by successive probes over an initial disturbance, so as to select, when convergence is reached, a solution having a behavior or stability which is adapted to downstream conditions. The scheme in figure 16 shows that the initial disturbance ϵ was conventionally produced on the pressure in subcritical cases, whereas it was produced over the initial position of the pressure jump and thus enabling the solution to cross a critical point located farther downstream, in the most supercritical cases, and without singularities.

In practice, such a resolution is extremely difficult and lacks generality. It is virtually unachievable as soon as the region where the strong interaction begins, i.e. the disturbance region, is not known in advance, or as soon as successive strong interactions are present, a fortiori if they mutually interfere with each other.

/11

5.4. Pseudo-Unsteady Methods

The first important improvement was suggested by Werle-Vatsa [67 to 69] for simple wave type external supersonic flows in which the nonviscous calculation is reduced to a simple local algebraic relationship between the pressure and direction of the flow. By means of a slip coupling over the displacement surface, we obtain :

$$p_x = - \beta \delta_{xx}^* \quad (5.2)$$

Werle-Vatsa's basic idea was simply to replace the coupling problem with a fictitious problem of variation obtained by replacing the term δ_{xx}^* with $[\delta_{xx}^* - \delta_t^*]$, and calculating the asymptotic state when $t \rightarrow \infty$ using a numerical method of alternating directions with two steps, the first being implicit in (y, t) , the second in (x, t) . If we consider, for example, the equation of motion in x which contains the only unsteady term:

$$\rho u u_x = \rho v u_y = \beta [\delta_{xx}^{**} - \delta_t^*] + [\varepsilon u_y]_y \quad (5.3)$$

we obtain schematically to pass from time n to time $(n+1)$:

$$\left. \begin{aligned} [\rho u u_x + \rho v u_y]^{n+1} &= \beta \left[(\delta_{xx}^{**})^n - \frac{2}{\Delta t} (\delta^{n+1} - \delta^n) \right] + [\varepsilon u_y]_y^{n+1} \\ [\rho u u_x + \rho v u_y]^{n+1} &= \beta \left[(\delta_{xx}^{**})^{n+1} - \frac{2}{\Delta t} (\delta^{n+1} - \delta^n) \right] + [\varepsilon u_y]_y^{n+1} \end{aligned} \right\} \quad (5.4)$$

The first half time step leads to a conventional calculation of the boundary layer where δ_{xx}^{**} , and therefore p_x is applied. It is resolved upstream to downstream, as the linearization of the equations calls on the preceding time step introduced to avoid singular behaviors at the separations. The second half time step is reduced to:

$$\beta (\delta_{xx}^*)^{n+1} - \beta (\delta_{xx}^*)^n = \frac{2}{\Delta t} [\delta^{n+1} - 2\delta^{n+\frac{1}{2}} + \delta^n] \quad (5.5)$$

which leads to the simple resolution of the tridiagonal

matrices for δ^{*n+1} , after discretization. The method was extended by Napolitano, Werle, Davis [69] to semi-unlimited incompressible external flows within the framework of laminar triple-deck equations. In this case, the algebraic relationship (5.2) should be replaced by a Cauchy integral (5.6) which makes the half-time step more complex (5.7):

$$\delta_{xz}^* = \frac{1}{\pi} \oint_{-\infty}^{+\infty} \frac{f_{\xi}}{x-\xi} d\xi \quad (5.6)$$

$$(\delta_{xz}^*)^{n+1} = \frac{1}{\pi} \oint_{-\infty}^{+\infty} \frac{f_{\xi}^n + \frac{1}{2} \frac{d}{dt} [\delta_{xz}^{*n+1} - 2\delta_{xz}^{*n} + \delta_{xz}^{*n-1}]}{x-\xi} d\xi \quad (5.7)$$

After discretization (5.7) leads for δ^{*n+1} to an algebraic system exhibiting a full matrix, but with diagonal dominance. A relaxation iteration is therefore necessary, in incompressible flows, to solve the second half time step by successive inversions of simple tridiagonal matrices.

A quite different pseudo-unsteady method was suggested by Briley, McDonald [70] and was used by Gleyzes, Cousteix, Bonnet [71] to calculate short transitional separation bulbs of leading edges, in incompressible flows, using a simplified local strong coupling approach. The basic idea was to use real unsteady equations of the boundary layer, while retaining the steady inviscid flow equations. The resolution is also pseudo-unsteady, to the extent where the boundary layer is calculated from the nonviscous pressure field of the preceding instant, the inviscid flow being adjusted a posteriori as a steady flow under the most recently calculated displacement effect. This simple technique is still justified only by the obtainment of asymptotic steady solutions when $t \rightarrow \infty$.

5.5. Direct Or Inverse Methods Of Relaxation

This principle of this class of methods lies on a more

rigorous formulation and on an extension of conventional iterative methods, used to improve the weak coupling techniques at the cost of a few successive approximations over the displacement thickness.

The strong coupling is obtained here for a rigorous convergence of the successive decoupled resolutions of the inviscid flow and unsteady boundary layers problems, while excluding any arbitrary smoothing technique. The stability of the iteration is controlled by sub-relaxation [3, 13, 39, 72, 73]. The linkage of the segmented viscous and nonviscous calculations is quite convenient and leads to a broad generality of use in subsonic, transonic or supersonic states. The downstream influence on the upstream in supersonic flows may be obtained automatically [3, 13, 15], as in pseudo-unsteady techniques, by directly applying the appropriate boundary conditions downstream, whether strong successive mutually interfering interactions, or streams not reducing to a simple wave are involved. The counterpart of this generality appears, for certain cases, in the preliminary calculations required for the coupling iteration. However, experience has shown [3, 13, 15, 39, 77] that this coupling iteration may be easily compete with those required to calculate inviscid flows, in the case of subsonic or transonic relaxation methods. In this case, the coupling iteration appears as an explicit relaxation technique for the viscous boundary condition (5.1) applied to inviscid flows, and the increased computer costs associated with viscosity is limited. /12

Considering that relationship (5.1) becomes identified with a boundary layer resolution, the coupling iteration, called direct or inverse, depending on whether we are solving for the cycle $(n+1)$ a direct or inverse type nonviscous problem:

$$\text{Direct :} \quad \theta^{n+1} = \frac{A_2}{A_1} \delta^* \left[\frac{dp}{dx} \right]^n + \frac{A_3}{A_1} \quad (5.8)$$

$$\text{Inverse :} \quad \left[\frac{dp}{dx} \right]^{n+1} = \frac{A_1}{\delta^* A_2} \theta^n - \frac{A_3}{\delta^* A_2} \quad (5.9)$$

For the direct method, if we assume that the inviscid flow is an operator which relates a pressure $p^{n+1}(x)$ to a given angular distribution $\theta^n(x)$, the inclusion of (5.8) leads to operator F related to the iteration of the overall fixed point:

$$\theta^{n+1}(x) = F[\theta^n(x)] \quad (5.10)$$

Likewise, when A_1 may be reduced to zero owing to a separation, the resolution (5.8) should be avoided and, assuming that an inverse inviscid flow operator correlates $\theta^n(x)$ with the data of $p^n(x)$, by adding relationship (5.9), integrated in x , we obtain an inverse fixed point iteration;

$$p^{n+1}(x) = G[p^n(x)] \quad (5.11)$$

The adoption of one of the two techniques (5.10) (5.11), or even their joint use in an alternating combined method (5.10) or (5.11) as a function of the predefined regions on boundary Ox , were used by Lock [39], Lineberg, Steger [74], Le Balleur [61, 72], Carter [73], Melnik, Chow, Mead [26, 29], among many other authors. In all of these cases, the method was stabilized by a large sub-relaxation ω , independent from x , determined without any other criterion than the previous numerical experience:

$$\theta^{n+1}(x) = \theta^n(x) + \omega \{ F[\theta^n(x)] - \theta^n(x) \} \quad (5.12)$$

The lack of generality of the previous approach was, however, eliminated by the present author through a study of approximated stability [13] permitting a local calculation

of $\omega(x)$. The study shows that operator F of (5.10), linearized around $\theta''(x)$, appreciably implies that the harmonic distributions of disturbance $[\theta(x) - \theta''(x)]$ are specific functions and that the corresponding approximation of the specific complex values of F is μ_0 , that of G being μ_1 with:

$$\mu_0 \cdot \mu_1 = 1 \qquad \mu_0 = \frac{\alpha \tilde{B} \delta^*}{\sqrt{1 - M^2}} \qquad (5.13)$$

M designates the local Mach number of the nonviscous flow, α the harmonic frequency, \tilde{B} is a parameter of viscous form related with B' in (4.11), or (A_2/A_1) in (5.1). The highest specific value $\mu_0(x)$ or $\mu_1(x)$ makes it possible to determine $\omega(x)$, highly dependend upon x like μ_0 or μ_1 (see [13]), while a local over-relaxation is not to be excluded.

If $R(\alpha)$ and $I(\alpha)$ designate the real and imaginary parts of μ_0 for example, the stability of (5.12) will be obtained if:

$$\omega(x) \leq 2 \omega_{opt}(\alpha_{max}) \qquad \omega_{opt} = \frac{1-R}{(1-R)^2 + I^2} \qquad \alpha_{max} = \frac{\pi}{\Delta x} \qquad (5.14)$$

In the direct case (5.10), a discretization step, small Δx increases the highest frequency α of the possible disturbances and reduces the value of $\omega(x)$ in the direct problem (5.10), while ω must be zero at separation or re-attachment points where $A_1 = 0$, $\tilde{B} \rightarrow \infty$, $\mu_0 \rightarrow \infty$. In inverse mode (5.11), however, the cancellation of μ_1 leads to these points at $\omega = 1$.

Numerically, the local calculation of $\omega(x)$ shows that the direct mode relaxation (5.10) is well conditioned for attached boundary layers, the inverse relaxation on the pressure (5.11) is also near separated layers or when it

is close to being near separated layers.

5.6. Implicit Linearized Method

Besides the dual nature of the preceding behavior, physically related to a dominant influence of the inviscid flow or the boundary layer for the pressure determination, depending on whether the boundary layer is more attached or more separated, the fact that there is a stronger recourse to a sub-relaxation when Δx is smaller shows the explicit nature of the method (5.10) as well as the probable advantage of a more implicit method. The idea of a Newton method for solving the discretized equation (5.10) was suggested by Burne, Rubbert, Nark [60]. Accordingly, for each iteration, we must determine the inviscid flow P_{ij}^n and the boundary layer B_{ij}^n influence matrices. They are expressed if we select for variables $p(x)$ and $\delta^*(x)$, discretized in p_i and δ_i^* in the inviscid flow, in \bar{p}_i and $\bar{\delta}_i^*$ in the boundary layer:

$$\left. \begin{aligned} p_i - p_i^* &= P_{ij}^* (\delta_j^* - \delta_j^{*n}) \\ \bar{\delta}_i^* - \bar{\delta}_i^{*n} &= B_{ij}^* (\bar{p}_j - \bar{p}_j^*) \end{aligned} \right\} \quad (5.15) / 13$$

For iteration $(n+1)$ we may therefore adopt the solution of the linearized coupled problem which is expressed in the form of a matrix:

$$\left. \begin{aligned} p^{n+1} = \bar{p}^{n+1} &= p^n + (I - P^n B^n)^{-1} [P^n (\bar{\delta}^{*n} - \delta^{*n}) + P^n B^n (p^n - \bar{p}^n)] \\ \delta^{n+1} = \bar{\delta}^{n+1} &= \delta^{*n} + B^n [(p^n - \bar{p}^n) + (p^{n+1} - p^n)] \end{aligned} \right\} \quad (5.16)$$

If the nonlinear effects on P_{ij}^n and B_{ij}^n are weak, the convergence must be rapid. Each iteration is still complex, requiring the inversion of a full matrix $[I - P^n B^n]$

and above all an estimate of the influence matrices P^n and B^n , a priori a costly evaluation within the framework of finite differences methods, particularly in transonic flows. Little information is currently available about this method, although its use is indicated by Thiede [54]. A very similar technique is described by Arieli, Murhpy [76] for pseudo-direct calculations of the boundary layer.

5.7. Semi-Inverse Relaxation Methods

From the practical standpoint, the complexity of the method described above as well as the mixed type relaxation iterative methods (direct or inverse by regions) leads us to suggest [3, 13 to 15, 75] a new relaxation iteration for separated boundary layer regions or those on the verge of reaching this state. This method may be qualified as semi-inverse in that only the boundary layer problem is processed in inverse mode, the given data being either the direction of the external flow $\theta^n(x)$, or the displacement thickness $\delta^{*n}(x)$. As shown in figure 17, $\theta^n(x)$ gives a double pressure predictor for each iteration, one given by the inviscid flow $p^n(x)$, the other given by the boundary layer $\tilde{p}(x)$, the problem being to correct $\theta^n(x)$ iteratively so that $p^n(x)$ will converge near $\tilde{p}(x)$.

An approximated stability analysis of the direct or inverse coupling iterations described in paragraph 5.4 enabled us to offer a solution to this problem. We may notice that if the correction selected $[\tilde{\theta}^{n+1}(x) - \theta^n(x)]$ is such that the disturbance $[p^{n+1}(x) - p^n(x)]$ in the inviscid flow is exactly $[\tilde{p}(x) - p^n(x)]$, the new distribution $\theta^{n+1}(x)$ is identical to the result of an inverse calculation of the inviscid flow subjected to $\tilde{p}(x)$. The chainage of such an inverse calculation simulated for the inviscid flow and a true inverse calculation for the boundary layer, therefore reproduces iteration (5.11) and may be stabilized like it,

by a local calculation of a relaxation coefficient $\omega(x)$, according to (5.13) (5.14). The analysis must still be completed by an appropriate technique in order to solve the problem of small inverse disturbances, of the Prandtl-Glauert type, enabling $[\tilde{\theta}''(x) - \theta''(x)]$ to be calculated from $[\tilde{p}(x) - p^n(x)]$. We have shown [13] that a harmonic analysis makes it possible to reduce each frequency mode α to a local algebraic relationships whose association with the relaxation (5.13) (5.14) leads us to the following corrections, if $U^n(x)$ and $\tilde{U}(x)$ designate the velocities related to the pressures $p^n(x)$ and $\tilde{p}(x)$:

$$\begin{aligned} \text{Subsonic points:} \quad \theta'' - \theta^* &= \frac{\delta^* B \sqrt{1-M^2}}{\alpha \delta^* B - \sqrt{1-M^2}} \left[\frac{1}{U} \frac{d\tilde{U}}{dx} - \frac{1}{U^*} \frac{dU^*}{dx} \right] \\ \text{Supersonic points} \quad \theta'' - \theta^* &= \frac{\delta^* \tilde{B} \sqrt{M^2-1}}{\alpha^2 \delta^* \tilde{B}^2 + (M^2-1)} \left[\frac{1}{U} \frac{d^2 \tilde{U}}{dx^2} - \frac{1}{U^*} \frac{d^2 U^*}{dx^2} \right] \end{aligned} \quad (5.17)$$

by adopting $\alpha_{max} \alpha = (\pi/\Delta)$, the dependency of the preceding local corrections on θ^* with respect to α are finally eliminated. Among other advantages, the semi-inverse iteration (5.17) requires only a detection of the coupling errors on the pressure gradient. As a result, it can easily be alternated with the direct iteration (5.12) as a function of the local form parameter of the viscous layer, without ever leading to discontinuous pressure distributions during the course of the convergence, for any number of regions resolved in inverse mode, or for any modifications made during the iterations.

For example, this combined method was used to calculate the supersonic separation on a compression bar, in a laminar or turbulent flow, on the assumption of a simple wave, by solving a well-defined problem directly with a zero pressure gradient at the last calculation point, figures 18 and 19. It was also applied to calculate symmetrical transonic airfoils in theories of small disturbances with shock or leading edge separation and to capture numerically the strong interaction at the base of a shock over a fine mesh, figures 20 to 22.

A semi-inverse slightly different correction was suggested by Carter [78] more recently. For each iteration, the correction is made of the displacement thickness $\delta^{*n}(x)$ and not of the angular direction of the flow. In the incompressible case, for example, the correction $\theta^*(x)$ is expressed in a local algebraic form:

$$\delta^{*n+1} = \Omega \delta^{*n} \left[\frac{U}{U^n} \right] \quad (5.18)$$

in which Ω is a relaxation coefficient, even over-relaxation coefficient ($1 < \Omega < 2$). This method was recently used by Kwon, Pletcher [79], Whitfield et al. [80].

It is interesting to note that there is an analogy between (5.18) and (5.17) in the subsonic case. If we assume, for example, that the coupling is obtained by inclusion of the displacement thickness, or $\theta = (d\delta^*/dx)$, the derivation of (5.18) directly gives:

$$\theta^{*n+1} - \theta^* = \frac{d\delta^{*n+1}}{dx} - \frac{d\delta^{*n}}{dx} = \Omega \delta^* \left[\frac{1}{U} \frac{d\tilde{U}}{dx} - \frac{1}{U^n} \frac{dU^n}{dx} \right] \quad (5.19)$$

The rigorous identity of the formulations (5.17) (5.18) should therefore be obtained for the incompressible case, if $\Omega = [B\Delta x / \pi\delta^*B - \Delta x]$. The analogy (5.17) (5.19) also shows the ambiguity of the notion of over-relaxation or subrelaxation in (5.17) (5.18), the subrelaxation in figure 17 occurring in (5.17) only at the concept level, the over-relaxation Ω of (5.18) being weighted by the multiplicative factor δ^* .

Finally, let us recall that the use of non-automatized semi-inverse type techniques was first mentioned by Kuhn [81, 82].

5.8. Semi-implicit Methods

Recent trials have been carried out to develop methods which are partially free of the explicit nature of the relaxation techniques described in paragraphs 5.5 and 5.7, but leading to simpler solutions than Newton's method in paragraph 5.6.

A first analysis was suggested by Veldman [83] in the case of unlimited incompressible flows for which the rate of disturbance induced on the viscous layer is given by a homologous Cauchy integral of (5.6), if the coupling is obtained by a distribution of sources on the wall:

$$u - u_0 = \oint_{-\infty}^{+\infty} \frac{v}{x - \xi} d\xi \quad v = \frac{d}{d\xi} (u \delta^*) \quad (5.20)$$

After the discretization, the velocity distribution u_i or pressure distribution p_i becomes associated, by virtue of (5.20) with the displacement thickness distribution δ_i^* by a linear form whose coefficients A_{ij} , predominantly diagonal, can be calculated directly. We may express:

$$\text{Inviscid flow: } p_i^{n+1} - A_{ij} \delta_i^{*n+1} = \sum_{j < i} A_{ij} \delta_j^{*n+1} + \sum_{j > i} A_{ij} \delta_j^{*n} \quad (5.21)$$

Schematically, the boundary layer appears in a discrete form like an appreciably lower triangular matrix operator B_{ij} :

$$\text{Boundary Layer: } \delta_i^{*n+1} - B_{ii}^{n+1} p_i^{n+1} = \sum_{j < i} B_{ij}^{n+1} p_j^{n+1} + \sum_{j > i} B_{ij}^n p_j^n \quad (5.22)$$

It is clear that the iteration indices n and $(n+1)$ were selected in (5.21) and (5.22) so that a resolution worked out from upstream to downstream may implicitly solve the first members in station i , the second members being known, according to a Gauss-Seidel type technique.

Like the Gauss-Seidel technique, the method (5.21) (5.22) can also be over-relaxed.

A second semi-implicit analysis developed by Wai, Yoshihara [84] for calculations of transonic airfoils in a small disturbance approximation. The potential problem:

$$(1 - M_\infty^2 - \lambda \phi_x) \phi_{xx} + \phi_{yy} = 0 \quad (5.23)$$

$$\phi_y(x, 0) = f(x) + \bar{H}(x) \quad (5.24)$$

is solved, in the inviscid flow where $\phi(x)$ by the Murman-Cole relaxation method, implicit column-wise along y , semi-implicit or implicit in x , depending on the decentering applied to ϕ_x and ϕ_{xx} . In the inviscid flow, the boundary layer behavioral relationship (5.1) gives:

$$\phi_y(x, 0) = f(x) + b(x) \phi_{xx} + c(x) \quad (5.25)$$

a relationship in which $b(x)$ and $c(x)$ should be calculated by the other boundary layer equations. If this calculation is performed from upstream to downstream while scanning the columns at the same time for ϕ , it is clear that (5.25) (5.23) may be solved simultaneously in semi-implicit mode, exactly like for inviscid flows, with the same discretization for ϕ_y and ϕ_{xx} . The main advantage is that the interactive treatment (5.25), even when discretized in semi-implicit mode for ϕ_{xx} , the improvement being that of a Gauss-Seidel technique, in analogy with (5.21) (5.22).

The simultaneous relaxation of the integral boundary layer equations and of the stream function, through successive implicit scannings by columns, was also indicated by Moses, Jones, O'Brien [85] in the case of separated subsonic flows. It is used by Ghose, Kline [86] in the calculation of diffusers.

6. SYNTHESIS EXAMPLE - CALCULATION OF AIRFOILS

Among the methods of calculating compressible flows of viscous fluids past airfoils, using coupling methods like those used in the approximations in paragraphs 4 and 5,

we may mention those of Bavitz [37], Bauer, Korn [38], Lock, Collyer, Firmin, Jones [39], Melnik, Chow, Mead [29], Wai, Yoshihara [84], Nandanam, Stanewsky, Inger [40], Le Balleur [15], such a list not being limitative. We are not interested here in the comparative performances of the methods from a practical standpoint, most still being the subject matter of current developments and generally providing more accurate results than currently usable Navier-Stokes solvers [87]. What we are looking for here is simply an example of a synthesis calculation, directly usable in applications, combining various viscous interactions mutually influencing each other (trailing edge, shock-boundary layer interaction, separation), and revealing the development of methods for an effective treatment of strong couplings and those offering a complete enough methodology to completely describe the viscous flow at high Reynolds number, in a direct extension of numerical techniques developed for inviscid flows.

6.1. Bavitz, de Bauer, Korn et al. Methods

In these first methods of calculating airfoils in viscous flows, the approximations used for the coupling are still close to the weak coupling methods. The wake is still not taken into account. The displacement effect of the boundary layers is obtained by altering the airfoil design geometry after adding the displacement thickness. The stabilization and convergence of the coupling iterations are relatively uncertain and incorporate smoothings or extrapolations of $\delta^*(x)$, an empirical processing of the trailing edge region being used as a compensation in the Bavitz method. The inviscid flow is calculated using the potential Garabedian, Korn method. The nonconservative form is most often preferred owing to a certain error compensation because the viscous effects at the base of the shock are not taken into account, the mesh being selected so as to

extend the compression under the shock far enough to avoid any separation in the boundary layer calculation [37].

6.2. Collyer, Lock et al. Methods

The investigation of more complete methods for strong interacting phenomena was initiated by Lock and his associates by first solving the inviscid flow using small disturbances transonic techniques, figure 23, then using Garabedian's and Korn's potential method, and this was independently of the practical performances of the analyses mentioned above. Figure 23 recalls that the wake effects were introduced in the form of a normal velocity jump, corresponding to the displacement effect (3.5) and in the form of a tangential velocity or pressure jump associated with the wake curve effect of the type (4.13). The curve of the stream lines under consideration is still a mean curvature. Furthermore, in the case of the complete potential equation, the wake conditions are applied to a mesh line and not to the viscous wake itself. The separations are not processed.

Compared to the preceding methods, the main improvements besides treating the wake are that the normal velocity on the airfoil wall is processed to determine the displacement effect without altering the design geometry, the simultaneous iteration on the viscous effects and on the potential calculation, the replacement of the smoothing techniques on δ^* with a uniform viscous sub-relaxation, determined empirically without altering the solution when convergence is reached. The latter improvement consisted of simulating as close as possible the pressure jumps of the shock waves provided by the potential calculation, by weighting the conservative and nonconservative numerical techniques. No special viscous processing was introduced for the shock-boundary layer interaction.

6.3. Melnik, Chow, Mead Method

Like the method just described, this analysis is applied to airfoils free of separations, based on the Green integral method of boundary layer and wake calculations, and does not introduce any special processing for the strong interaction at the base of the shock waves. Figure 24 recalls that, excluding the trailing edge region, the viscous boundary conditions applied to the inviscid flow are similar to the method of Lock et al., the conditions on the wake always being applied to a slightly different line than that of the real wake.

The improvement of the methods consists of using the Jameson potential calculation in a conservative form, and using a sophisticated processing of the strong turbulent interaction at the leading edge: the latter is based on an asymptotic multi-deck analysis, figure 25, and guarantees a rational behavior of the model at the infinite limit of the Reynolds number. From the practical standpoint, we should notice in figure 25 that the viscous calculation model incorporates a non-irrotational normal pressure gradient in the external layer. This is expressed in the potential calculation by a local modulation of the traditional coupling boundary conditions at the leading edge, figure 24. It generally leads to overvalued pressure jumps on the wake in the immediate vicinity of the trailing edge.

6.4. Nandaman, Stanewsky, Inger Method.

This method is simpler than the two preceding ones, except for the processing of the shock-boundary layer interaction. It uses the Jameson potential method, in a conservative and nonconservative form, as well as an integral method for the boundary layer. The wake is not computed.

The separations are not processed. The coupling is obtained by altering the design geometry of the airfoil by adding a displacement thickness subjected to a large smoothing, particularly in the shock region.

The method would therefore be comparable to those described in paragraph 6.1., if a more sophisticated processing of the shock-boundary layer interaction were not incorporated. The latter appears as a separate module whose role is to determine as accurately as possible the state of the boundary layer after the shock, and to provide a more realistic estimate of the pressure on the wall in the shock region. This module is based on Inger's non-asymptotic multi-deck analysis [88]. The results are better if the compression applied to the Inger module, theoretically that of a straight shock, is that of a maximum deflecting oblique shock. /16

6.5. Wai, Yoshihara Method

The method is a recent development and is used for the potential flow of a simple small transonic small disturbances calculation. The boundary layer and the wake are calculated using an integral method, including separations. The first feature consists of a simultaneous resolution of the potential small disturbances equations and of the viscous boundary condition (5.1), during the relaxation by column associated with the Murman-Cole technique. This process, elicited in paragraph 5.8, is semi-implicit in that the scanings per columns must be repeated to assure the convergence. Conversely, the interactive processing of the viscous calculation eliminates the singularity problems at the separation.

The second feature of the method is to replace the modelization, called viscous ramp modelization, with an

integral calculation of the boundary layer in the shock region, in the case of separation, in the absence of resolving the strong coupling with a fine enough mesh. The modelization schematically consists of establishing a ramp for the displacement surface with an angle which corresponds to a predetermined recompression level on a shock polar, where the empiricism leads to the selection of an intermediary value between the sonic deviation and the maximum deviation [89]. This modelization of δ^* is necessary not only for improving the comparison with the experiment, but also to assure the convergence of the calculation.

6.6. Le Balleur Method

The method uses for the inviscid flow the potential calculation of Chattot, Coulombeix, Tomé [90] which solves the equation in a conservative form, with the Jameson artificial viscosity. The boundary layer, laminar or turbulent, as well as the wake are calculated with an integral method including the reverse flows, the wake being calculated with or without the dissymetry effect. The matching formulation of paragraph 4.3 for the inviscid flow leads to boundary conditions on the wall and on the wake which are similar to those of Lock et al. or of Melnik et al.. Yet the geometry of the wake line is here still periodically dapted during the calculation to coincide with the mean viscous wake line. The method does not provide any special processing of the leading edge, but strictly observes here the strong coupling associated with the matching formulation. The curvature effect applied (4.13) incorporates the averaged estimates of $K(x)$, which are distinct for the upper and lower half-wakes.

The coupling is achieved by a direct or semi-inverse relaxation iteration, as a function of the instantaneous local form parameter of the viscous layer. This iteration, described in paragraphs 5.5 and 5.7, is comparable to that

used for calculating the inviscid flow, figure 26. The pressure gradient along the wall is estimated in the inviscid flow using centered schemes for subsonic flows, and decentered downstream for supersonic flows. The boundary layer transition at the wake is assimilated with a continuous process for the inviscid flow as well as for $\delta^*(x)$, but discontinuous for the viscous calculation. The method automatically captures the modification brought to the pressure distributions by the viscosity in the immediate vicinity of the trailing edge, provided that the meshes are approximately the local thickness of the viscous layer, whether there is a separation or not.

Figures 27 to 32 show the use of the method at low velocities and at high incidences, for the NACA 0012 airfoil. On this airfoil, the calculation approaches the stall incidence, with a 70% upper surface separation from the chord and a reattachment in the wake. In the present state of the method's development, this calculation at an incidence of 16° is possible only by observing the wake dissymetry, figures 27 and 31 show the aspect ratio change associated with its mean line. Figures 39 to 41 show by the plotting of the stream lines and of the iso-Mach lines that the calculation method restores not only the distant inviscid flow, but also the mean viscous flow in detail.

Figures 33 and 34 show the use of the method in subcritical transonic cases on the RAE 2822 airfoil, tested by Cook, McDonald, Firmin [91]. In supercritical transonic cases, in contrast to the calculations made in the small disturbances approximation, figures 20-21, it remains currently impossible to numerically capture the strong interaction at the base of the shock waves on a fine mesh adapted to the local boundary layer thicknesses, owing to the numerical difficulties of solving the potential equation

on such meshes. Without this complete resolution of the local viscous coupling, the compression under the shock is overestimated by the conservative method applied to the inviscid flow.

To correct this problem, an approached method was defined for the shock-boundary layer interaction. As figure 36 schematizes, this method simply consists of solving a local fictitious interaction on an enlarged scale ε_2 , compatible with the mesh. This is a homothetic image of the real scale interaction ε_1 , obtained by simple expansion of the local thickness δ of the viscous layer in the ratio $(\varepsilon_2/\varepsilon_1)$, yet without altering the Reynolds number $R\delta$. The strong coupling made over the fictitious interaction region ε_2 leads, on the one hand, to a more realistic interactive estimate of the boundary layer thickness, and on the other hand, to an expected reduction in the recompression level, as shown in figure 37. In contrast, the processing is essentially an approximation in that the alteration undergone by the inviscid flow in region ε_2 is inconsistent with the overall calculation scale C . For this, a quality numerical solution will therefore be maintained only if $\varepsilon_2 \ll C$, and even $\varepsilon_2 \ll L$, L representing the extent of the supersonic pocket. It may be observed in figure 38 that, thanks to the single viscous coupling effect, the calculation predicts a Mach number, after a shock which is slightly less than unity, which is closer to the experiment. It may also be observed that the numerical structure of the shock of the potential calculation is replaced by a continuous viscous compression, which is relatively spread out owing to the mesh used, figure 37. Figures 42 to 44 show the appearance of the iso-Mach lines and of the stream lines in the calculated viscous flow.

A spectacular effort has been made over the past few years in the inviscid flow region with a view to reinforcing the effectiveness and generality of the calculation techniques. It is important to stress first the major valorization resulting in practice from the coupling of these techniques with complementary viscous calculations, provided, however, that too restrictive approximations of the weak coupling are avoided. Changes in the methods of predicting local and overall wing and airfoil characteristics shows this trend.

In this light, we may note the conjunction of progress made of an analytical nature on interactive viscous calculations of fundamental phenomena such as trailing edge flows, thin layer separations, boundary layer - shock interactions, with progress made of a numerical nature, consisting mainly of developing new original strong coupling techniques. These improvements have made it possible to go beyond the stage of processing specific or local phenomena, and to synthesize computer means adapted to the complex flows encountered in industrial applications which compete with overall methods for direct resolutions of the viscous flow.

Yet, it is clear that the two approaches to phenomena of viscous interaction, the overall approach and the strong coupling approach, are actually more complementary than competitive. The current selection of relatively simple viscous approximations in the coupling methods is actually guided only by the concern to use coarser discretization meshes than those which are indispensable in the overall approach for numerically solving viscous layers and sub-layers. Coupling methods using simple viscous equations, and particularly those of Navier-Stokes type calculations,

produce in practice the minimum mesh densities compatible with the numerical resolution of strong coupling phenomena. Such densities, are between those used in inviscid flows and those of the Navier-Stokes type calculations, and lead to an economy which may be taken advantage of for calculating more complex flows, incorporating for example multiple viscous interactions or three-dimensional phenomena.

For less restrictive meshes, the progress made in the overall approach has obvious effects on the calculation of viscous regions in the method of coupling by regions. Finally, it is also conceivable to use Navier-Stokes solvers in the coupling methods replacing current inviscid flow calculations and on analogous meshes. Such a technique would make it possible, in three-dimensional flows, for example, to capture the macroscopic viscous phenomena by a local resolution of the Navier-Stokes equations with a turbulence model, whereas the concentrated phenomena of thin layers near the walls, their interaction with the external flow as well as their impact on the generation of vortex sheets would continue to benefit from less costly processings, through extensions of integral interactive boundary layer methods currently developed for airfoils and wings with a large aspect ratio.

From the specific standpoint, then, a few salient ideas or requirements may be extracted from current coupling techniques:

(i) the implementation of strong interaction coupled calculations presents two relatively different methods. The first uses a concept of regions linked by their boundary conditions, with the possibility of directly incorporating existing modules of the Navier-Stokes type. The second is based on the notion of overlapping viscous and nonviscous calculation regions, with the possibility of developing original methods for solving Navier-Stokes equations using an equation scattering technique.

(ii) The necessary replacement of weak coupling approximations with a strong rigorous coupling leads to an imperative requirement to develop specialized numerical methods, raising problems that are at least as complex as those associated with numerical techniques for inviscid and viscous flows. This requirement became obvious for trailing edge, separation and shock-boundary layer problems. The analysis is especially not very developed for a coupling between the Euler and Navier-Stokes equations.

(iii) The processing of boundary layer - wave shock interactions seems to be one of the most delicate problems of the calculation techniques, not only due to the error range attached to the turbulence modelizations, but also due to the reduced scales which should be used locally, even for calculating inviscid flows in the case of coupling method using minimal meshes. Similar problems of multiple resolution scales are presented in viscous layer separations in the vicinity of leading edges.

(iv) Among the improvements made in calculating airfoils, the replacement of the Euler equations for the potential equation shall be examined, particularly for higher transonic flows, in the event of a separation generating under the shock, with the ultimate benefit of a direct application to internal flows. Calculation-experiment comparisons brought to light from the corrections of error ranges on windtunnel walls, should also be highly desirable for refining existing methods of calculation.

(v) Calculations of airfoils in extreme flows, near stall or separation states under the shock, for example, reveal the very strong sensitivity of the overall flow

to the precision of the viscous layer calculation from the very origin of the latter. The development of turbulence models is therefore very important, even in the simplified forms encountered in integral methods.

REFERENCES

- [1] Peyret R., Viviand H., "Computation of viscous compressible flows based on the Navier-Stokes equations," AGARD AG-212 (Sept. 1975). /18
- [2] Viviand H., "Processing of problems of inviscid flow - viscous flow interactions in compressible two-dimensional cases based on Navier-Stokes equations." VKI/AGARD LS 94, or "Three dimensional and unsteady separations at high Reynolds numbers" (Feb. 1978).
- [3] Le Balleur J.C., Peyret R., Viviand H., "Numerical studies in high Reynolds number aerodynamics," Symposium on Computers in Aerodynamics, Farmingdale (June 1979, Computers and Fluids, vol, 8, no. 1, p. 1-30 (March 1978).
- [4] Hollanders H., Viviand H., "The numerical treatment of compressible high Reynolds numbers flows." VKI Lecture Series on "The numerical treatment of fluid dynamics equations" (19-23 March 1979), T.P. ONERA 1979-22.
- [5] Murphy J.D., Presley, L.L., Rose W.C., "On the calculation of supersonic separating and reattaching flows," AGARD CP-168 (1975).
- [6] Steger J.L., "Implicit finite difference simulation of flow about arbitrary geometrics with application to airfoils," AIAA Paper no. 77-665 (1977).
- [7] Joncheray P., "Two-dimensional model for the formation of vortex sheets escaping from the lateral edge of a wing," PhD, University P. and M. Curie, Paris 6 (1977).
- [8] Brune G.W., Rubbert P.E., Foerster C.K., "The analysis of flow fields with separation by numerical matching," AGARD CP-168, (1975).
- [9] Seginer A., Rose W.C., "A numerical solution of the flow field over a transonic airfoil including strong shock-induced flow separation," AIAA Paper no. 76-330, San Diego (July 14-16, 1976).
- [10] Seginer A., Rose W.C., "An approximate calculation of strong interaction on a transonic airfoil, AIAA Paper No. 77-210, Los Angeles (January 24-26, 1977).
- [11] Rose W.C., Seginer A., "Calculation of transonic flow over supercritical airfoils sections.," "J. of Aircraft vol 15, no. 8, p. 514-519 (1978).
- [12] Le Balleur, J.C., "Viscous-nonviscous coupling" analysis of the problem including separations and shock waves," La Recherche Aeronautique, no. 1977-6, p. 349-358 Nov.1977) - ESA TT. 476 (1978).

- [13] Le Balleur J.C., "Viscous-nonviscous coupling: numerical method and application to two-dimensional transonic and supersonic flows," La Recherche Aérospatiale, No. 1978-2, p. 67-76 (March 1978).
- [14] Le Balleur J.C., "Viscous-nonviscous coupled calculations including separations and shock waves in two-dimensional flows," VKI/AGARD LS-94 on "Three dimensional and unsteady separation at high Reynolds numbers" (Feb. 1978).
- [15] Le Balleur J.C., Viviand H., "Methods of calculating separated two-dimensional flows at high Reynolds numbers", 16th AAAF Symposium, Lille (November 1979), ONERA Report No. 1979-145.
- [16] Dodge P.R., "Numerical method for 2D and 3D viscous flows, AIAA Journal, vol. 15, no. 7, p. 961-965, (July 1977).
- [17] Dwyer D.L., "Application of a velocity-split Navier-Stokes solution technique to external flow problems," 4th Computational fluid Dynamics Conf., AIAA Paper No. 79) 1449 (July 1979).
- [18] Johnston W., Sokol P., "A viscous-inviscid interactive compressor calculation," AIAA Paper no. 78-1140, (July 1978).
- [19] Briley W.R., McDonald H., "Analysis and computation of viscous subsonic primary and secondary flows", 4th Computational fluid dynamics conf. AIAA Paper no. 79-1453 (July 1979).
- [20] Dash S.M., Wilmoth R.G., Pergament H.S., "Overlaid viscous/inviscid model for the prediction of near-field jet entrainment," AIAA Journal vol. 17, no. 9, p. 950-958 (Spet. 1979).
- [21] Van Dyke M., "Perturbation methods in fluid mechanics," The parabolic Press (1975).
- [22] Mellor G.L., "The large Reynolds number asymptotic theory of turbulent boundary layers," Intern. J. of Engineering Sci., Vol. 10, pp. 851-873 (1972).
- [23] Melnik R.E., Grossman B., "Analysis of the interaction of a weak normal shock wave with a turbulent boundary layer, "AIAA Paper no. 74-598, Palo Alto (June 17-19, 1974).
- [24] Stewartson K., "Multistructured boundary layers on flat plates and related bodies. Advances in Appl. Mech., vol 14, pp. 145-239 (1974).

- [25] Melnik R.E., Chow R., "Asymptotic theory of two-dimensional trailing-edge flows," NASA SP 347, Part 1, Langley (March 4-6, 1975).
- [26] Chow R., Melnik R.E., "Numerical solutions of the triple deck equations for laminar trailing edge stall," Grumman Rept. RE-526J (October 1976).
- [27] Burggraf O.R., Rizetta D., Werle M.J., Vatsa V.N., "Effect of Reynolds number on laminar separation of supersonic stream," AIAA Journal vol. 17, no. 4, p. 336-343 (April 1979).
- [28] Melnik R.E., Grossman B., "Interaction of normal shock waves with turbulent boundary layers at transonic speeds," Grumman Rept. RE-517J (March 1976).
- [29] Melnik R.E., Chow R., Mead H.R., "Theory of viscous transonic flow over airfoils at high Reynolds number," AIAA Paper 77-680, Albuquerque (June 27-29), 1977).
- [30] Messiter A.F., "Interaction between a normal shock-wave and a turbulent boundary layer at high transonic speeds. Part I: pressure distribution," J. of Applied Math. and Physics (ZAMP), vol. 31, p. 227-246 (1980).
- [32] Ohrenberger J.T., Baum E., "A theoretical model of the near wake of a slender body in a supersonic flow," AIAA J., vol. 10, no. 9, pp. 1165 (September 1972).
- [33] Baum E., Denison M.R., "Interacting supersonic laminar wake calculations by a finite difference method," AIAA J., Vol. 5, no. 7, p. 1224 (July 1967).
- [34] Mahgoub H.E.H., Bradshaw P., "Calculation of turbulent inviscid flow interactions with large normal pressure gradients," AIAA Journal, Vol. 17, no. 10, pp. 1025-1029 (October 1979).
- [35] Patankar S.V., Spalding D.B., "A calculation procedure for heat, mass and momentum transfer in three-dimensional parabolic flows," Int.J. Heat Mass Transfer., Vol. 15, pp. 1787-1806 (1972).
- [36] Spalding D.B., "Numerical computation of steady boundary layers. A survey. Computational methods and problems in aeronautical fluid dynamics," London and New York Academic Press (1976).
- [37] Bavitz P.C., "An analysis method for two-dimensional transonic flow," NASA TN D.7718. (January 1975).

- [38] Bauer F., Korn D., "Computer simulation of transonic flow past airfoils with boundary layer correction." 2nd AIAA Comput. Fluid. Dyn. Conf., Harford (June 1975).
- [39] Collyer M.R., Lock R.C., "Prediction of viscous effects in steady transonic flow past an airfoil," Aero. Quart. Vol. 30, part 3 (Aug. 1979).
- [40] Nandan M., Stanewsky E., Inger G.R., "A computational procedure for transonic airfoil flow including a special solution for shock boundary layer interaction," AIAA Paper no. 8--1389 (July 1980).
- [41] Rehbach C., "Numerical calculation of unsteady 3D flow with vortex sheets," La Recherche Aerospatiale no. 1977-5, pp. 289-298 (September 1977).
- [42] Henderson M.L., "A solution to the 2-D separated wake modeling problem and its use to predict CL_{max} of arbitrary airfoil section," AIAA Paper no. 78-156 (January 1978).
- [43] Crocco L., Lees L., "A mixing theory for the interaction between dissipative flows and nearly isentropic streams." J. Aero. Scie., vol. 19, no. 10 (October 1952).
- [44] Goldstein S., "On laminar boundary layer flow near a position of separation," Quart. J. Mech. Appl. Math. 1, 43-69 (1948).
- [45] Cousteix J., Le Balleur J.C., Houdeville R., "Calculation of unsteady turbulent boundary layers in direct and inverse mode, including reverse flows. Singularities analysis." La Recherche Aerospatiale no. 1980-3, pp. 147-157 (May 1980).
- [46] Cousteix J., Houdeville R., "Singularities analogy in direct methods of calculating 3D steady and 2D unsteady boundary layers. Inverse modes analysis." AGARD Proceed. Symp. on Computation of viscous-inviscid interactions, Colorado Springs (September 29 - October 1, 1980).
- [47] Catherall D., Mangler K.W., "The integration of 2d laminar boundary layer equations past the point of vanishing skin friction." J.F.M., Vol. 26, part 1 (Sept. 1966).
- 48. Klineberg J.M., Steger J.L., "On laminar boundary layer separation," AIAA Paper no. 74-94, Washington (Jan. Febr. 1974).

/20

49. Carter J.E., "Inverse solutions for laminar boundary layer flows with separation and reattachment," NASA TR-R-447 (Nov. 1975).
50. Cebeci T., Keller H.B., Williams P.G., "Separating boundary layer flow calculations." J. of Comput. Physics 31, 363-378 (1979).
51. Pletcher R.H., "Prediction of incompressible turbulent separating flow." J. of Fluids Engineering, Vol. 100, p. 427-432 (December 1978).
52. East L.F., Smith P.D., Merryman P.J. "Prediction of the development of separated turbulent boundary layers by the lag-entrainment method." RAE-TR-77046 (March 1977).
53. Kuhn G.D., Nielsen J.N., "Prediction of turbulent separated boundary layers," AIAA Paper no. 73-663 (1973).
54. Thiede P.G., "Prediction method for steady aerodynamic loading on airfoils with separated transonic flow," AGARD-CP_204 (1976).
55. Delery J., Chattot J.J., Le Balleur J.C., "Viscous interaction with separation in transonic flow", AGARD CP-168 on "Flow separation", Gottingen (May 1975).
56. Garvine R.W., "Upstream influence in viscous interaction problems. The Physics of Fluids, vol. 11, p. 1413 (July 1968).
57. Weinbaum S., Garvine R.W., "On the two-dimensional viscous counterpart of the one-dimensional sonic throat," J.F.M. vol 39, pp 57-85 (1969).
58. King Non Tu, Weinbaum G., "A non-asymptotic triple-deck model for supersonic boundary layer interaction. AIAA J. vol. 14, no. 5, pp. 767-775 (June 1976).
59. Klineberg J.M., "Theory of laminar viscous-inviscid interactions in supersonic flow," Cal, Insti. Tech., PhD Thesis (May 1968).
60. Brune G.W., Rubbert P.E., Nark T.C., "A new approach to inviscid flow-boundary layer matching," AIAA Paper no. 74-601, Palo Alto (June 17-19, 1974).
61. Couston M., Angelini J.J., Le Balleur J.C., Girodroux-Lavigne P., "Inclusion of unsteady boundary layer effects in a 2D transonic calculation," Proceed. AGARD meeting on Boundary layer effects on unsteady airloads, Aix-en-Provence (17-18 Sept. 1980).

62. Lees L., Reeves B.L., "Supersonic separated and reattaching laminar flows," Pt I: General theory and application to adiabatic boundary layer-shock wave interaction," AIAA J., Vol. 2, No. 10 (1964).
63. Holt M., "Numerical methods in fluid dynamics," Springer-Verlag, Series in Computational Physics (1977).
64. Hankey W.L., Holden M.S., "Two-dimensional shock wave boundary layer interactions in high speed flows," AGARDograph AG-203 (June 1975).
65. Reyhner T.A., Flugge-Lotz, "The interaction of a shock-wave with a laminar boundary layer," Stanford Univ. Dir. of Eng. Mech. (November 1966).
66. Nielsen J.N., Lynes L.L., Goodwin F.K., "Calculation of laminar separation with free interaction by the method of integral relations, AFFDL TR-65-107 (June 1965).
67. Werle M.J., Vatsa V.N., "New method for supersonic boundary layer separations, AIAA J., vol. 12, no. 11 (November 1974).
68. Vatsa V.N., Werle M.J., "Quasi 3D supersonic viscous-inviscid interactions including separation effects," University of Cincinnati, Ohio, Tech. Rep. AFFDL-TR 75-138 (Sep 1975).
69. Napolitano M., Werle M.J., Davis R.T., "Numerical technique for the Triple-Deck problem," AIAA J. vol. 17, no. 7, pp. 699-705 (July 1979).
70. Briley W.R., McDonald H., "Numerical prediction of incompressible separation bubbles," J.F.M., vol. 69, pt 4, pp. 631-656 (1975).
71. Gleyzes C., Cousteix J., Bonnet J.L., "Laminar separation bulb with transition: theory and experiment," L'Aeronautique et l'Astronautique no. 1980-1 (Jan 1980).
72. Le Balleur J.C., Mirande J., "Experimental and theoretical study of 2D turbulent incompressible reattachment, AGARD-CP-168 on "Flow separation," Gottingen (May 1975).
73. Carter J.E., Wornom S.F., "Solutions for incompressible separated boundary layers including viscous-inviscid interaction," NASA SP-347, pp. 125-150 (1975).

74. Klineberg J.M., Steger J.L., "Calculation of separated flows at subsonic and transonic speeds," Proceed. of Intern. Conf. on Numerical Methods in Fluid Mech., Springer Verlag, vol. 11, pp. 161-168 (1973). /21
75. Le Balleur J.C., "Viscous interaction including turbulent boundary layer separation in two-dimensional flows," Communication Workshop on "Viscous interaction and boundary layer separation," Columbus, Ohio (July 1976).
76. Arieli R., Murphy J.D., "Pseudo-direct solutions to the boundary layer equations for separated flow," AIAA Paper no. 79-0139 (Jan. 1979).
77. Lock R.C., "Calculation of viscous effects on aerofoils in compressible flows," RAE Tech. Memo. Aero. 1646 (Sept. 1975).
78. Carter J.E., "A new boundary layer inviscid iteration technique for separated flow," 4th Computational fluid dynamics conf., AIAA Paper 79-1450 (July 1979).
79. Kwon O.K., Pletcher R.H., "Prediction of incompressible separated boundary layers including viscous-inviscid interaction," J. of Fluids engineering vol. 101, p. 466-472 (December 1979).
80. Whitefield D.L., Swafford T.W., Jacocks J.L., "Calculation of turbulent boundary layers with separation, reattachment and viscous-inviscid interaction," AIAA Paper no. 80-1439 (July 1980).
81. Kuhn G.D., Nielsen J.N., "Prediction of turbulent separated boundary layers," AIAA J., vol. 12, no. 7 (July 1974).
82. Kuhn G.D., "Calculation of separated turbulent flows on axisymmetric afterbodies including exhaust plume effects," AIAA J., vol. 18, no. 3, pp. 235-242 (March 1980).
83. Veldman A., Dijkstra D., "A fast method to solve incompressible boundary layer interaction problems", Proceed. of 7th Int. Conf. on numerical methods in fluid Dynamics, Stanford and NASA Ames (23-27 June 1980).
84. Wai J., Yoshihara H., "Viscous transonic flow over airfoils," Boeing Rep. D180-25934-1, and Proceed. of 7th int. Conf. on numerical methods in fluid dynamics, Stanford and NASA Ames (23-27 June 1980).

85. Moses H.L., Jones R.R., O'Brien W.F., "Simultaneous solution of the boundary layer and freestream with separated flow," AIAA J., vol. 16, no. 1, pp. 61-66 (Jan. 1978).
87. Swafford T.W., "Calculation of skin friction in 2D transonic, turbulent flows," ARO Inc., Sverdrup, AEDC-TR-79-12, Arnold Air Force Station (April 1979).
88. Inger G.R., "Upstream influence and skin friction in non-separating shock-turbulent boundary layer interactions," AIAA Paper no. 80-1411 (July 1980).
89. Magnus R.J., Yoshihara H., "Calculation of the transonic oscillating flap with "viscous" displacement effects," AIAA Paper no. 76-327 (1976).
90. Chattot J.J., Coulobieix, C., "Calculations of transonic flows past airfoils," La Recherche Aerospatiale, no. 1978-4, pp. 143-159 (July 1978), Vol C.
91. Cook P.H., McDonald M.A., Firmin M.C.P., "Aerofoil RAE 2822: pressure distributions, and boundary layer and wake measurements," AGARD-AR-138, Experimental data base for computer program assessment (1979).

COMPLETE NAVIER-STOKES EQUATIONS		
I. DIRECT RESOLUTIONS + EQUATION COMMUTATION	FILTERED N.S. EQ. + MODEL	{ OVERALL Approach COMMUTATION Method
	AVERAGED N.S. EQ. + MODEL	
	SIMPLIFIED AV. N.S. EQ.	
	.NS thin layer .Prandtl	

II. RESOLUTIONS: SEVERAL SYSTEMS + STRONG COUPLING	SEGMENTATION BY REGIONS + STRONG COUPLING	{ LINKING COUPLING Approach
	.Navier Stokes	
	.N.S. thin layer	
	.Prandtl	
	.Euler	
	SEGMENTATION BY EQUATIONS: (1) (2)	{ OVERLAPPING COUPLING Approach
	→ (1) INVISCID FL. } Strong Coupl.	
	→ (1) (2) VIS.FL. }	
	.Navier Stokes	
	.N.S. thin layer	
	.Prandtl	

III.	EULER + ISOBAR SEPARATIONS	{ Approximations of Intermediary Levels
	EULER + VORTICES	
	WEAK COUPLING EXTENSIONS	
	.A few iterations δ^*	
	.Modelized separations	

IV. RESOLUTIONS: WEAK COUPLING	N.S. PARABOLIC APPROXIMATIONS	
	.Upstream → Downstream	
	CONVENTIONAL BOUNDARY LAYER	
	.Inviscid fluid + Boundary Layer + 1 iteration δ^*	
	.Second order boundary layer.	

Figure 1 - Computation Methods In Viscous Fluids.

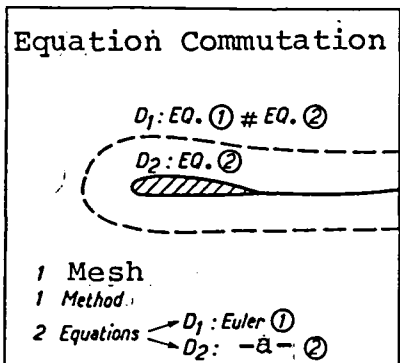


Fig 2 - Equation Commutation Method

Key: a-Viscous.

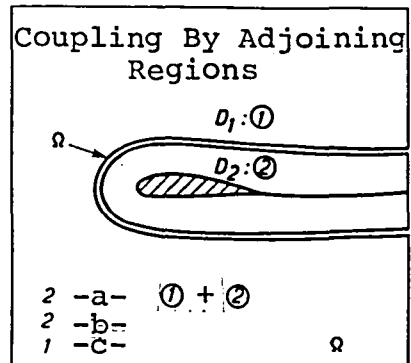


Fig 3 - Method of Coupling Along Adjoining Regions

Key: a-Methods; b-Disjoined meshes; c-Strong coupling;

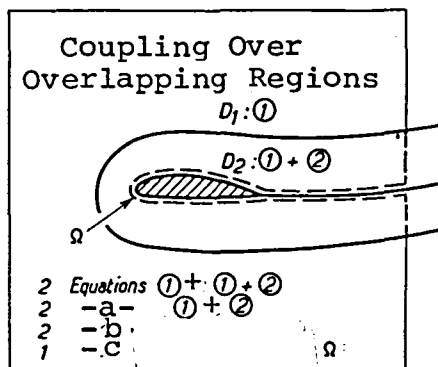


Fig 4 - Overlapping Coupling Approach

Key: a-Methods; b-Overlapping meshes; c-Strong coupling over Ω .

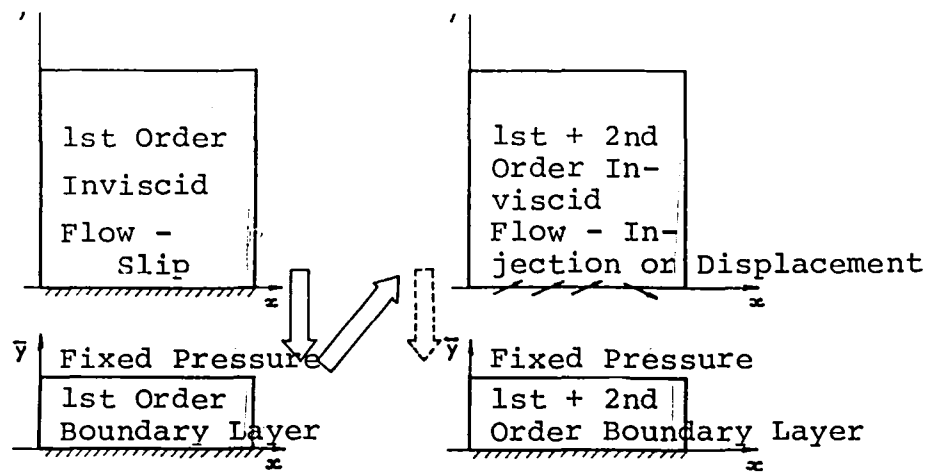


Figure 5 - Asymptotic Weak Coupling

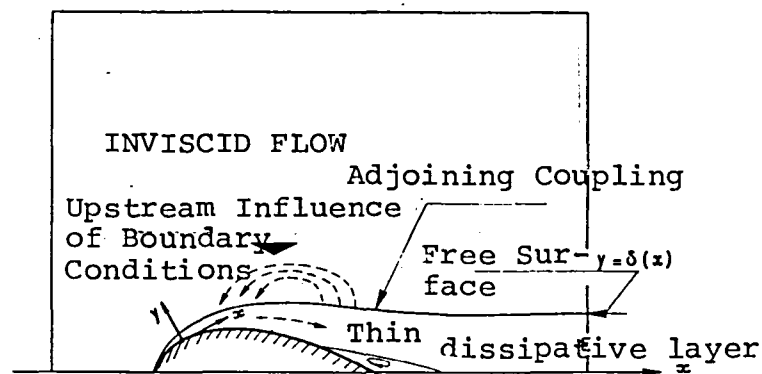


Figure 6 - Strong interacting Prandtl Layer - Coupling along adjoining regions (common boundaries).

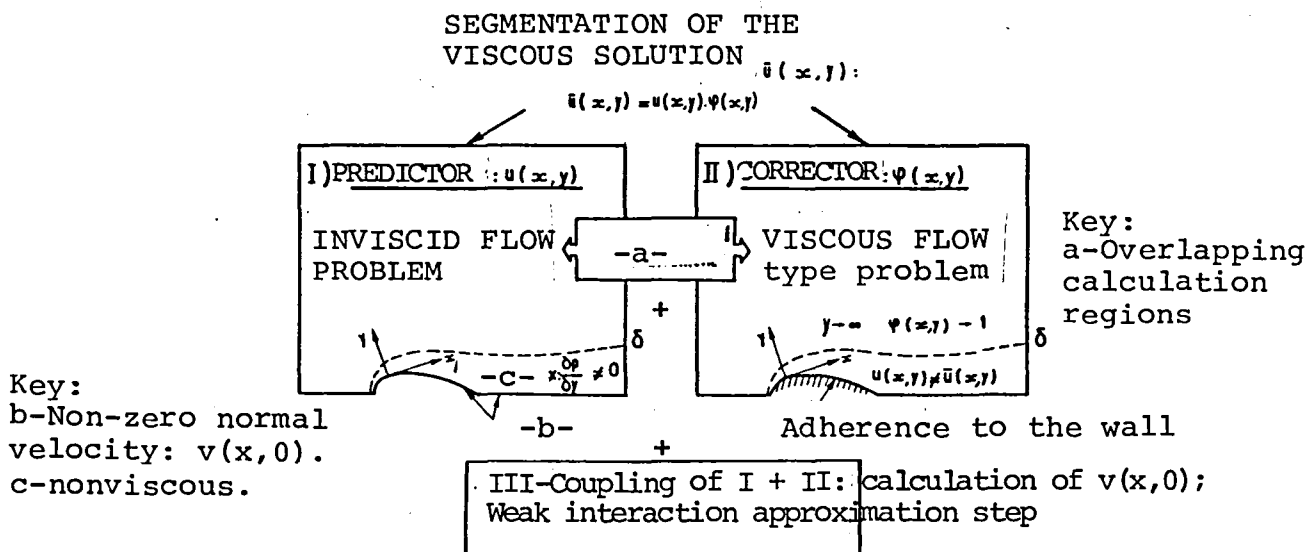


Figure 7 - Strong coupling of overlapping regions: matching formulation of the viscous calculation.

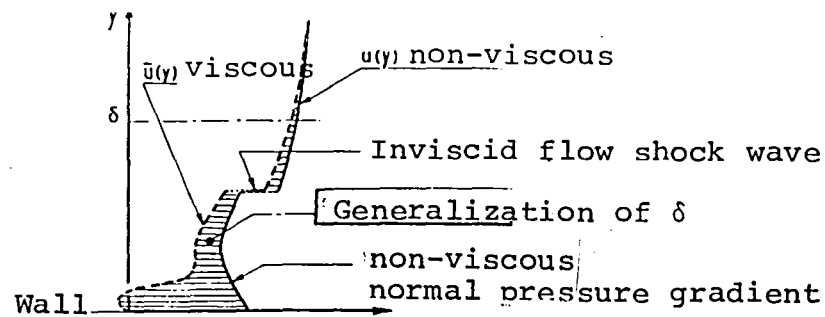


Fig 8 - Matching formulation: Scheme of viscous and non-viscous solutions for a given x-axis.

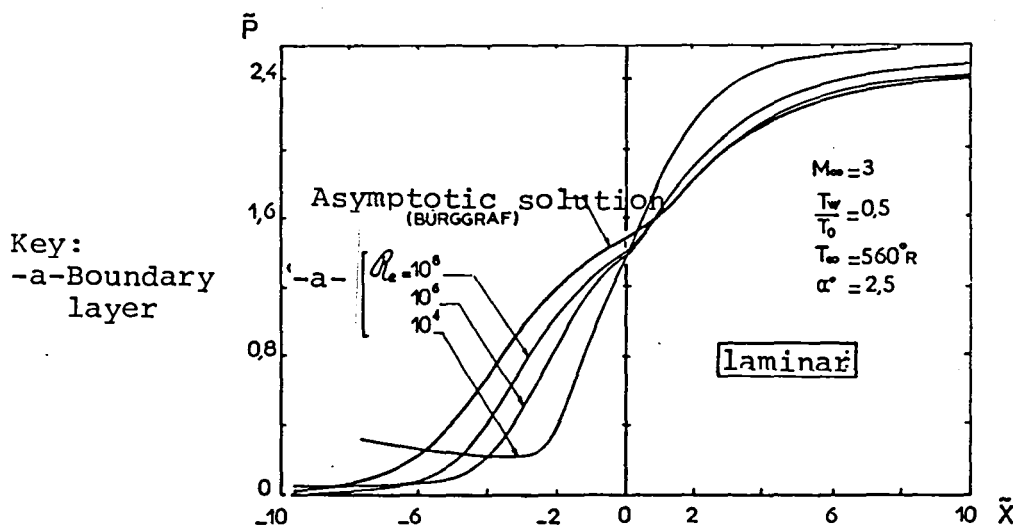


Fig 9 - Laminar supersonic ramp - Asymptotic behavior of the interacting Prandtl equations, according to Burggraf, Rizetta, Werle, Vatsse, ref. [27].

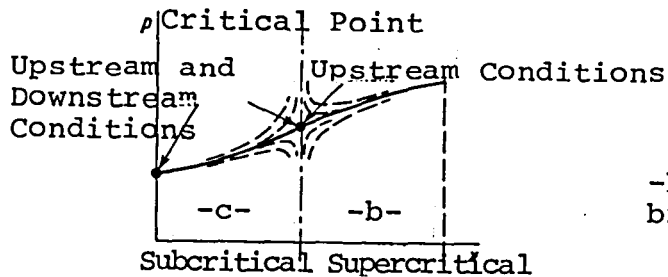


Fig 10 - Critical points in the Crocco-Lees sense.

Key: c-Unstable branchings;
b-Stable branchings.

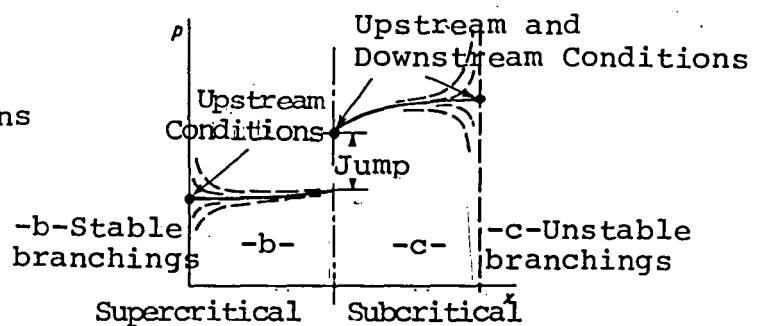


Fig 11 - Supercritical - Subcritical jumps.

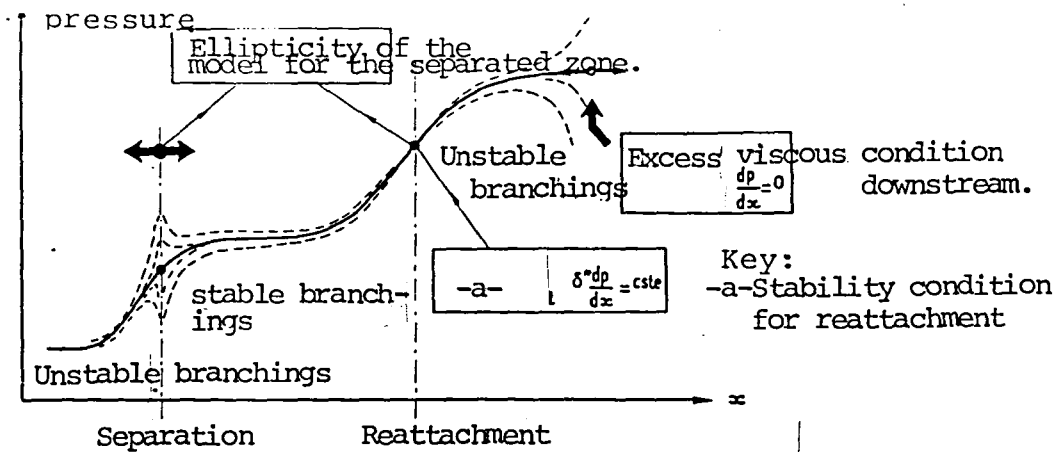


Fig 12 - Supersonic separation over a ramp. Diagram of the branching solutions for an initially subcritical layer.

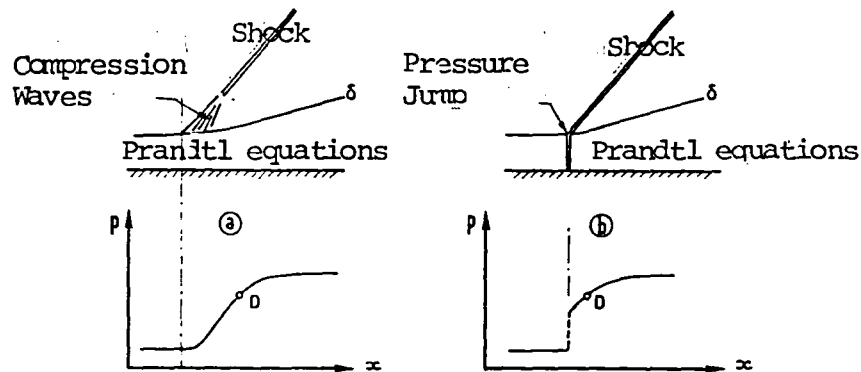


Fig 13 - Supersonic separation with the coupling model for adjoining regions: a) subcritical; b) supercritical.

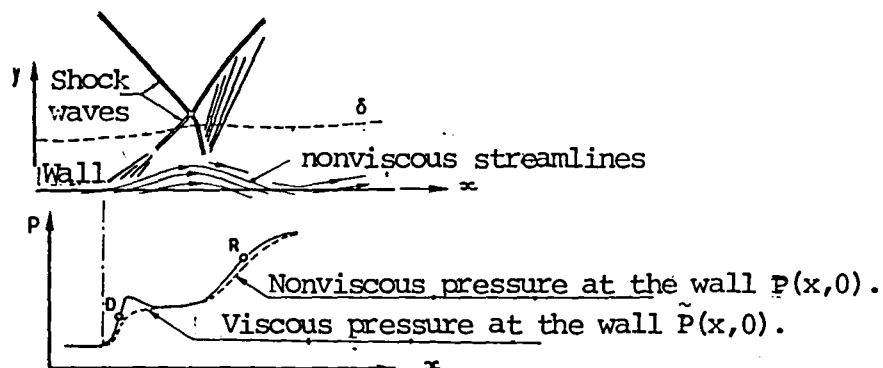


Fig 14 - Coupling of overlapping regions: nonviscous schematization of a supersonic turbulent separation. Pressure distribution at the wall.

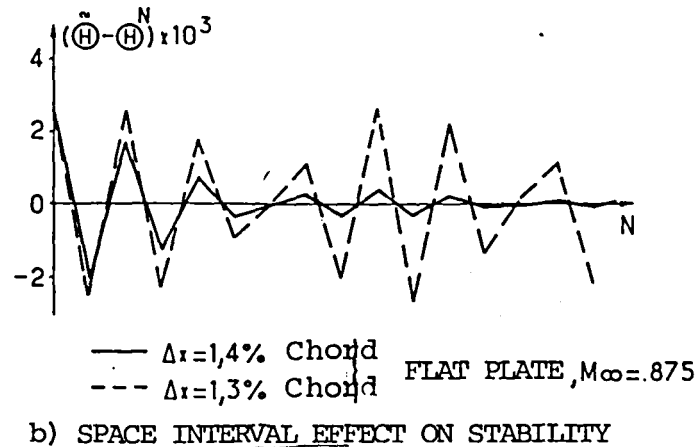
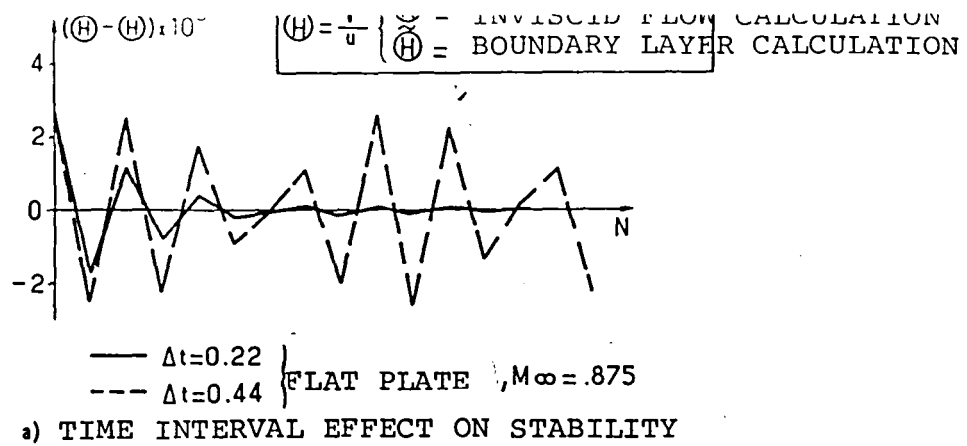


Fig 15 - Numerical instabilities of conventional coupling iterations on a flat plate in an unsteady flow as a function of Δx & Δt .

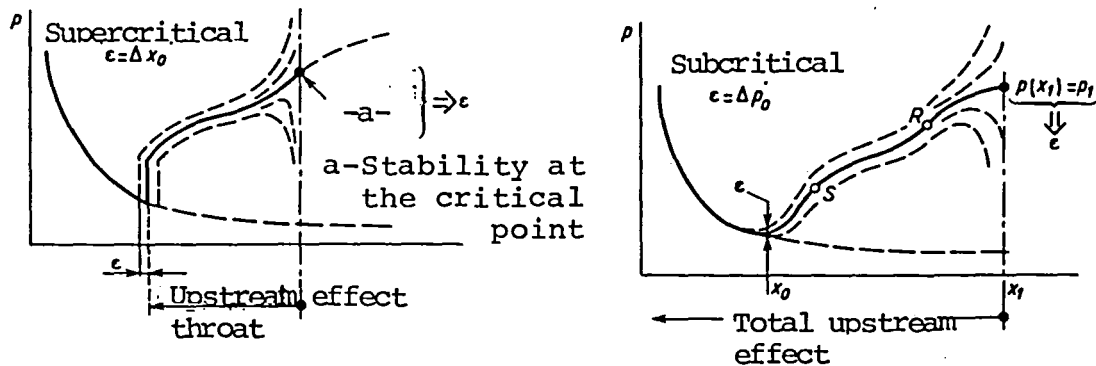


Fig 16 - Methods of initial conditions in supersonic flows.

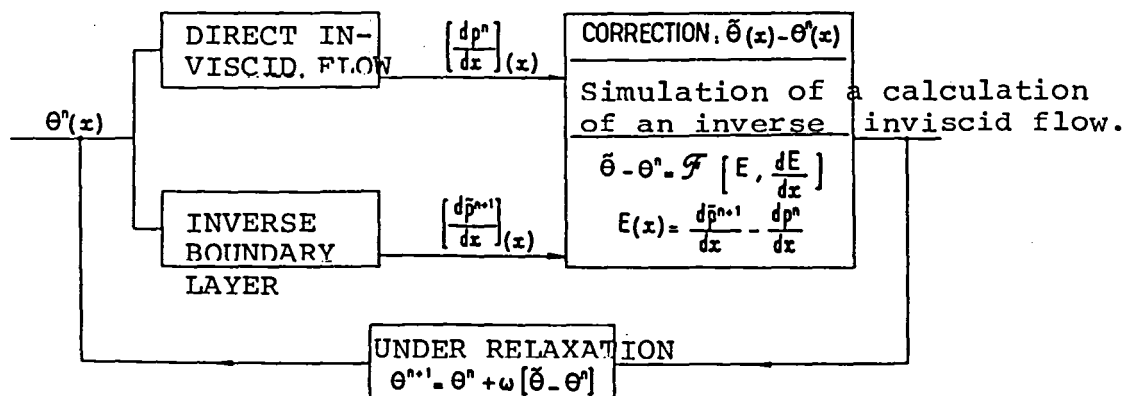
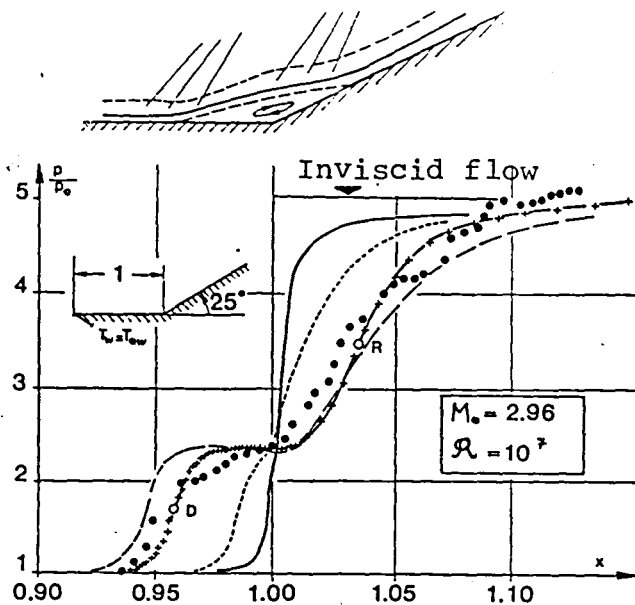
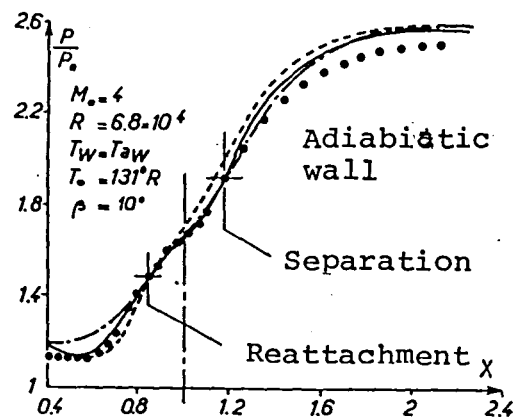


Fig 17 - Numerical method for a semi-inverse coupling



• Experiment: Law
 +++++ Present coupling method
 — Werle-Berte coupling methods
 - - - Equilibrium } N.S. Shang-Hankey
 - . - Turbulence



• Experiment: Lewis-Kühota-Lees
 - - - N.S. calculation: Carter
 — Werle-Vatsa coupling method
 - . - Present coupling method

Fig 18 - Turbulent supersonic separation on a ramp.

Fig 19 - Laminar supersonic separation on a ramp.

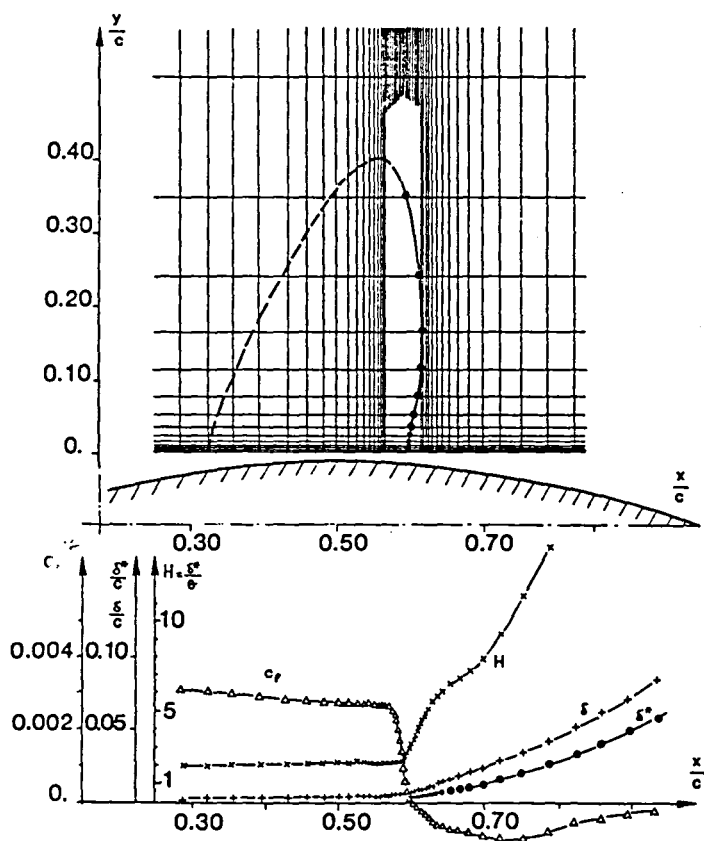


Fig 20 - Strong coupling calculation of a turbulent transonic separation under a shock of a circular symmetrical airfoil of 18%. $M = 0.788$ - $R = 4 \times 10^6$.

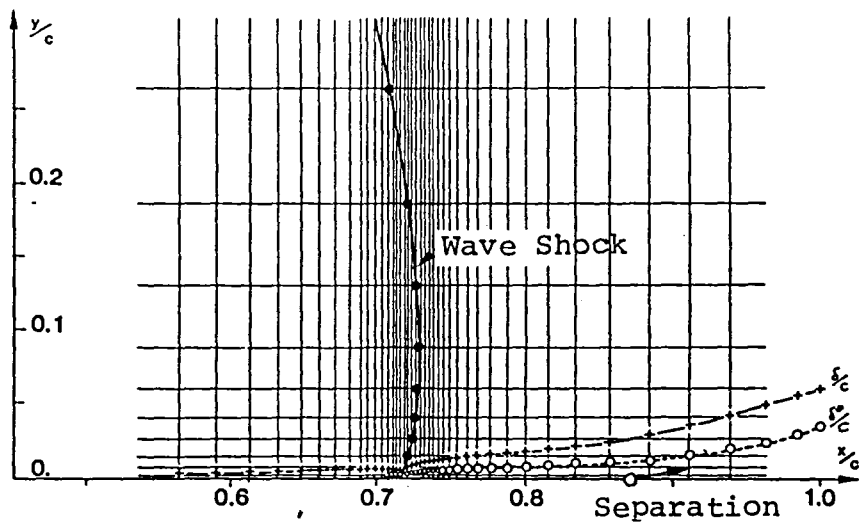
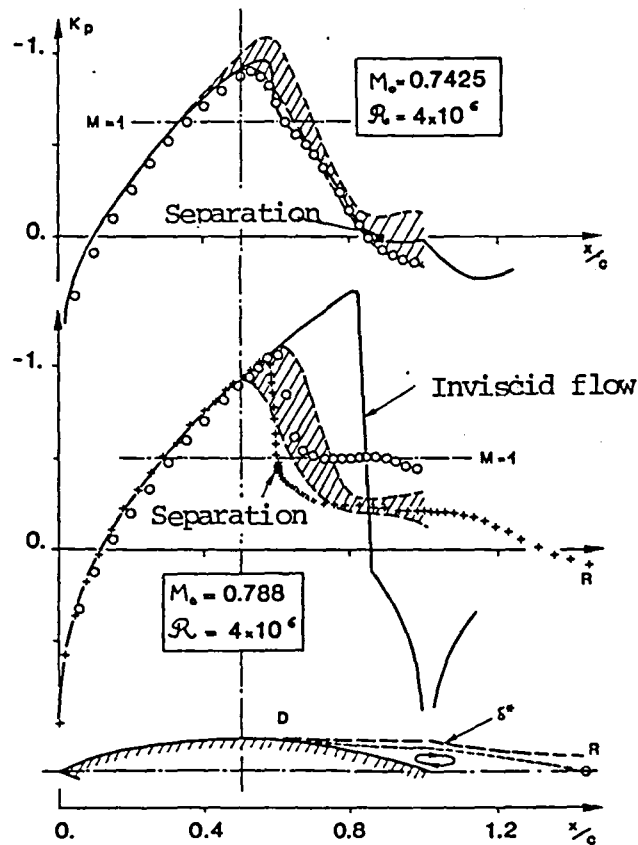


Fig 21 - Shock-boundary layer interaction region in a strong coupling calculation in small transonic disturbances. Viscous thicknesses.



o Experiment : Mc Devitt-Delwert

+++++ Present coupling method

////// N.S. Calculations: Delwart
(according to turbulence model)

Fig 22 - Symmetrical circular airfoil of 18% in small disturbance theory.

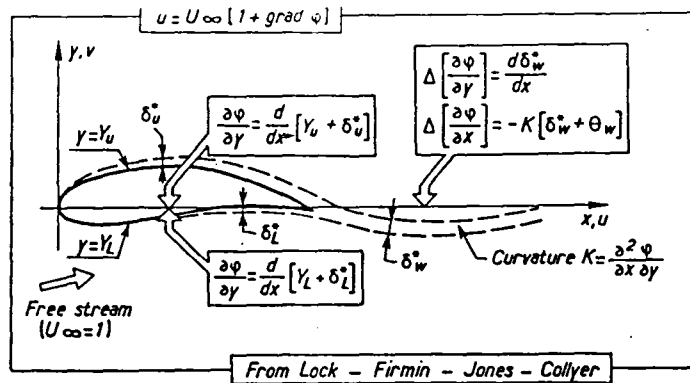


Fig 23 - Coupling calculation of airfoils in viscous flows: boundary condition of the inviscid flow, in small disturbances, according to ref. [77].

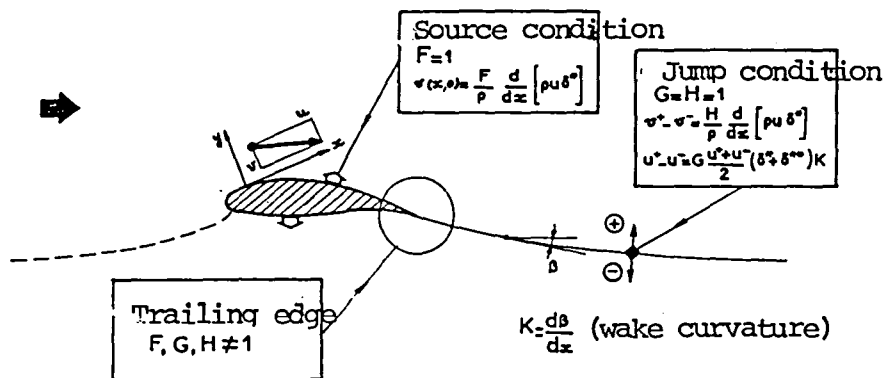


Fig 24 - Coupling calculation of airfoils in viscous flows: boundary condition of the inviscid flow according to Meinik, Chow, Mead, ref. [29].

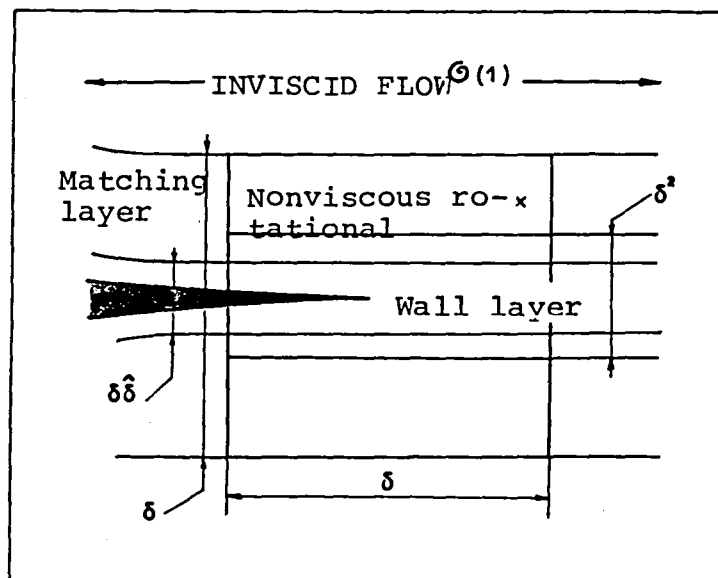


Fig 25 - Nonseparated turbulent trailing edge: asymptotic model by Melnik, Chow according to reference [29].

M : Mach number
 Θ : wall-velocity angle

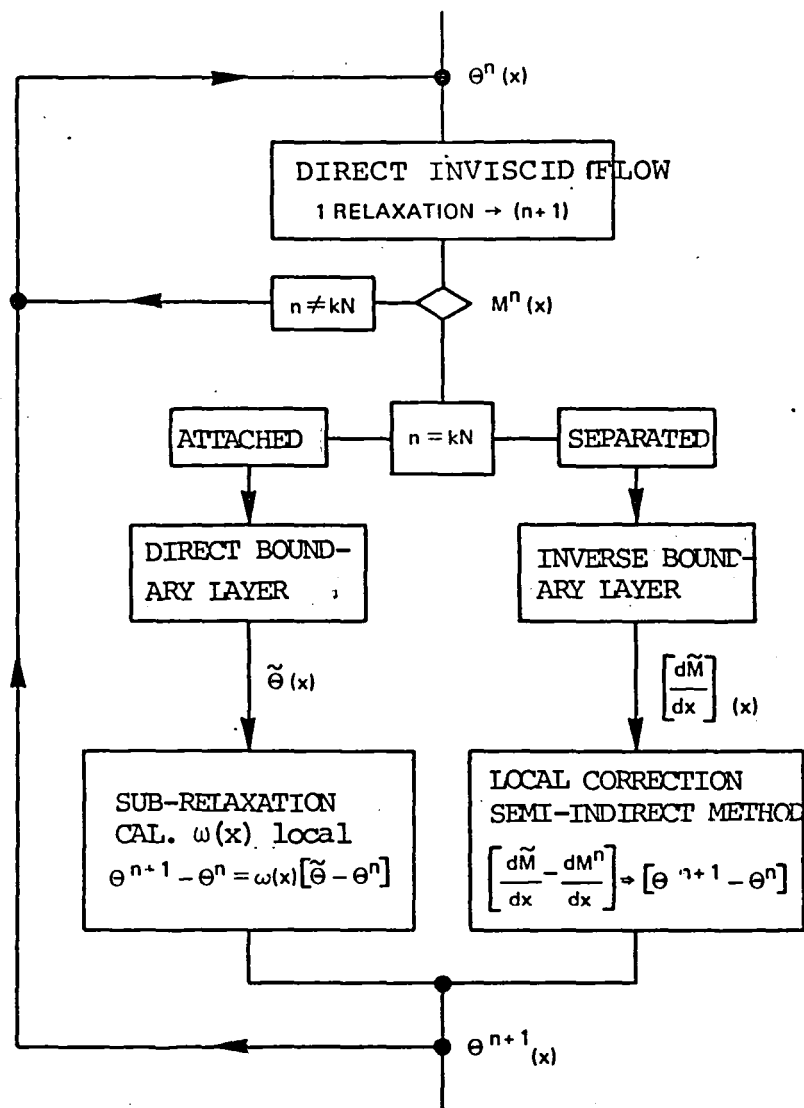
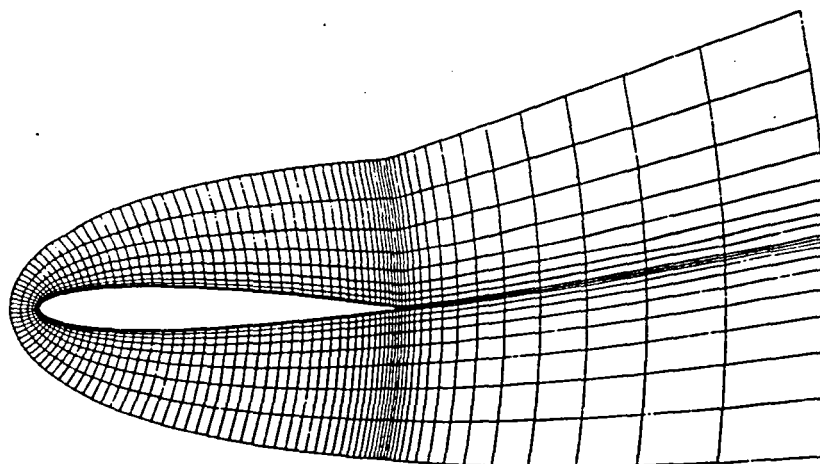


Fig 26 - Mixed relaxation method: direct or semi-inverse.



AIRFOIL, NACA0012 - $\alpha = 15^\circ$ - 145x21 Nodes

Fig 27 - Mesh with positioning of the wake in the symmetrical approximation.
 ($M = 0.116$, $\alpha = 15^\circ$, $R = 2 \times 10^6$).

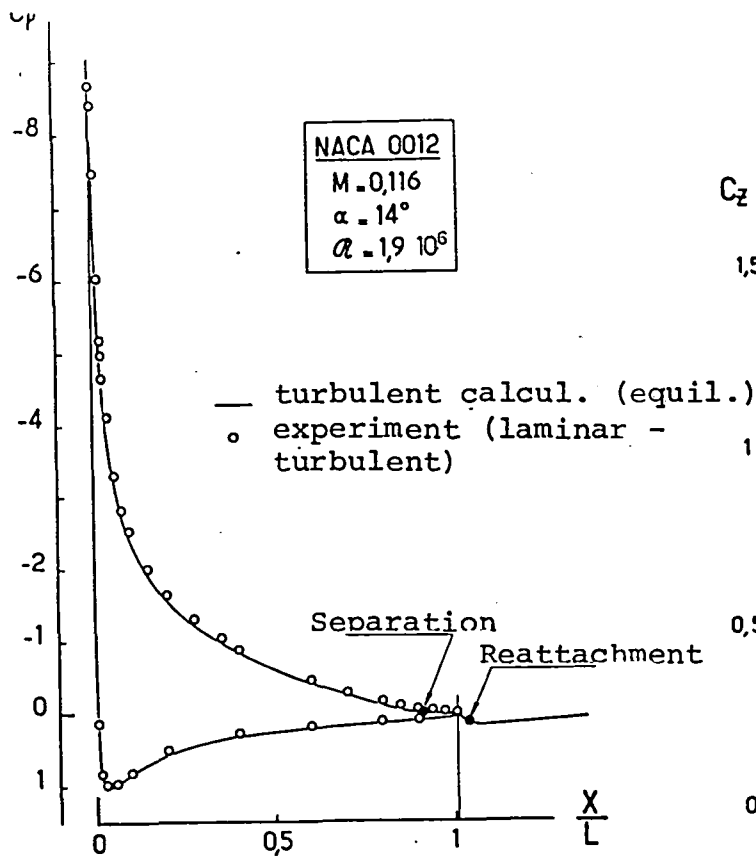


Fig 28 - NACA airfoil 0012
($V_o = 40$ m/s) turbulent coupled calculation.

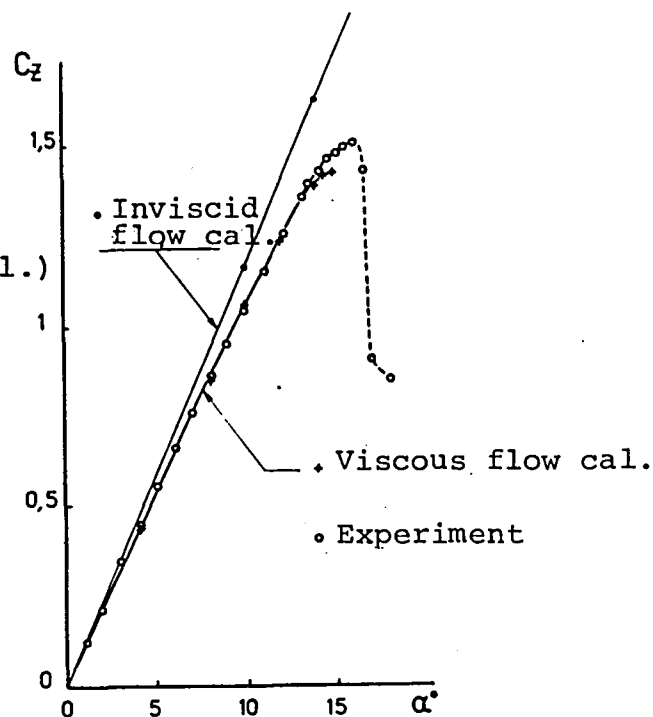


Fig 29 - NACA 0012 airfoil lift
 $V_o = 40$ m/s, $R = 1.9 \times 10^6$. strong coupling calculation (turbulent, symmetrical wake).

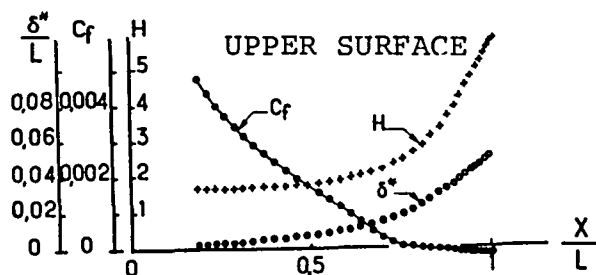
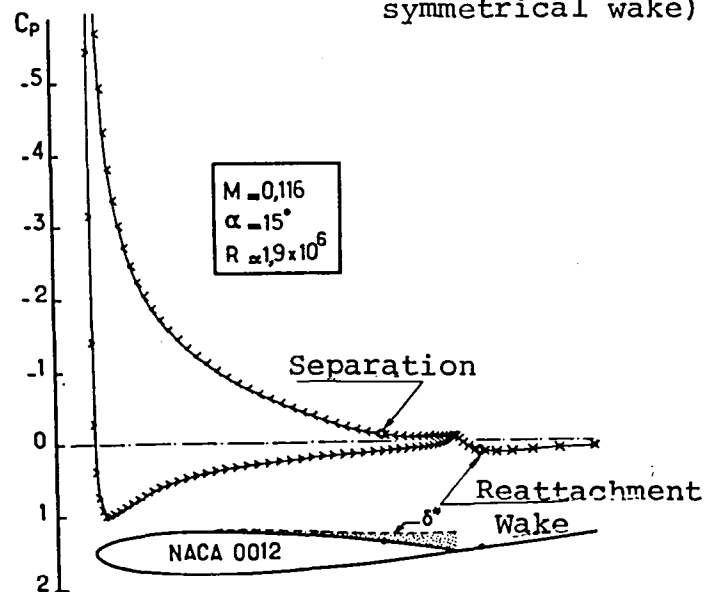
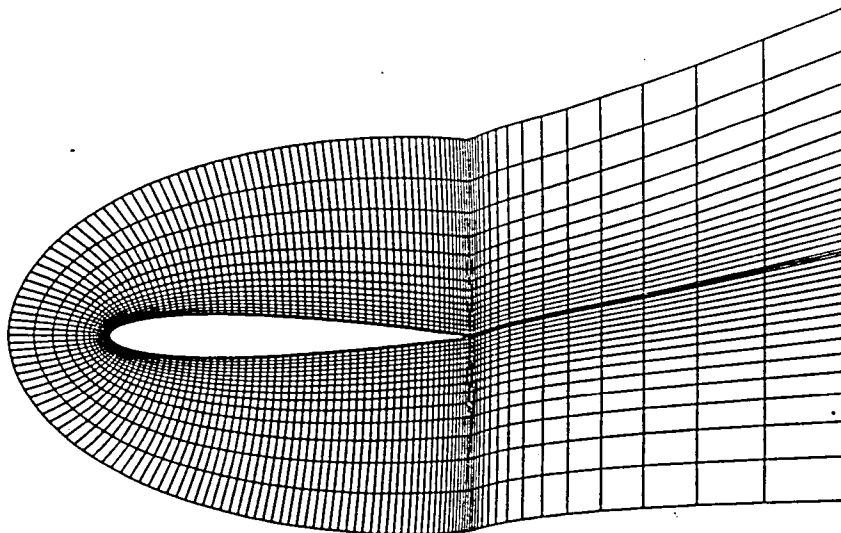


Fig 30 - Viscous effects at the trailing edge and pressure plateau. Coupled turbulent calculation, symmetrical wake.



NACA0012 I=16 - JCFOIL9 - 181X27

($M = 0.116$, $\alpha = 16^\circ$, $R = 2 \times 10^6$).

Fig 31 - Mesh with wake positioning in the dissymetrical approximation.

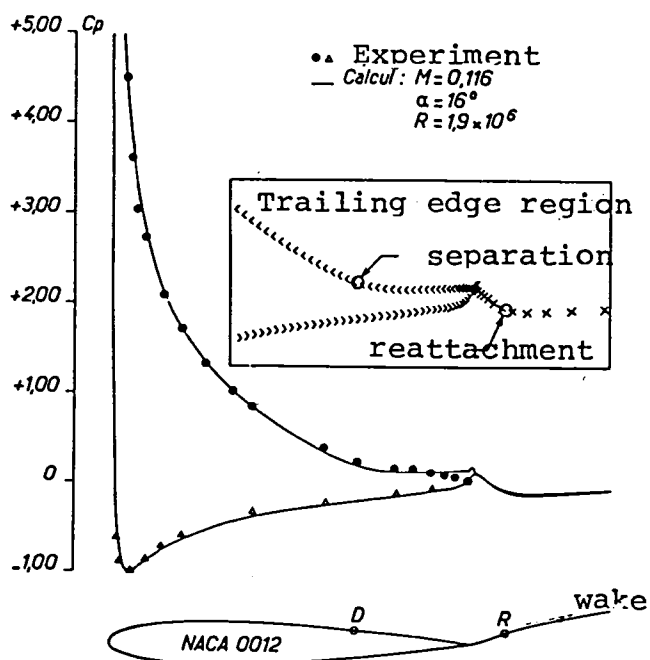


Fig 32 - Calculation of the NACA 0012 at high incidence with dissymetrical wake.

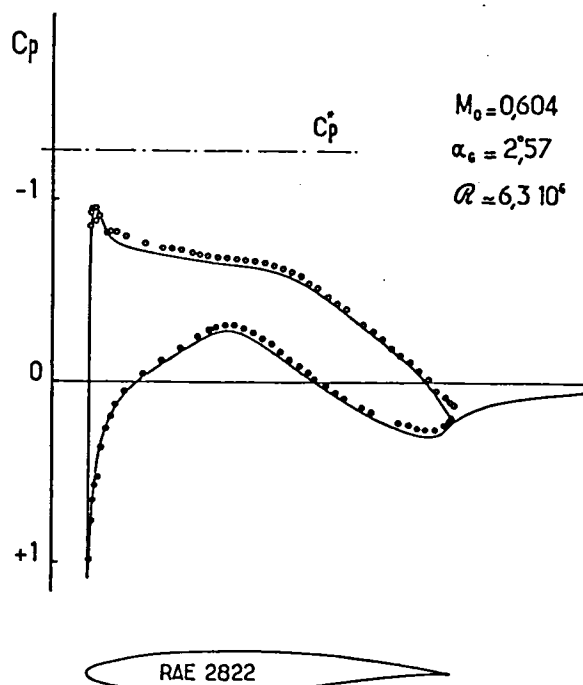


Fig 33 - Calculation of the RAE airfoil in a subcritical flow.

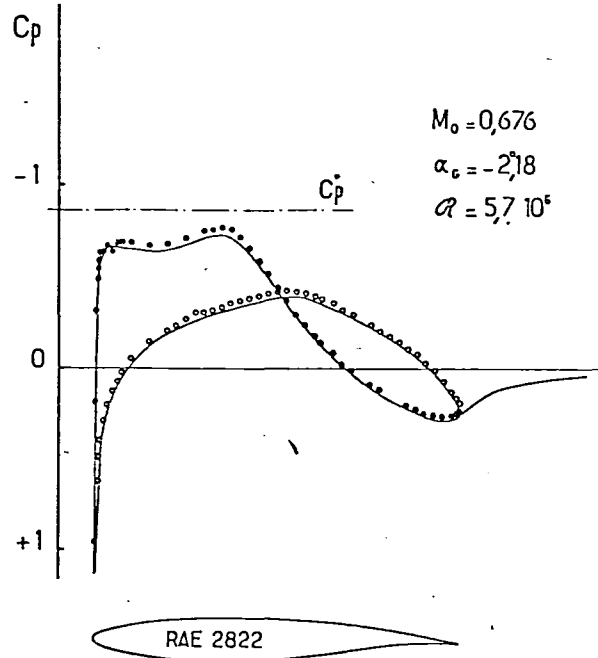
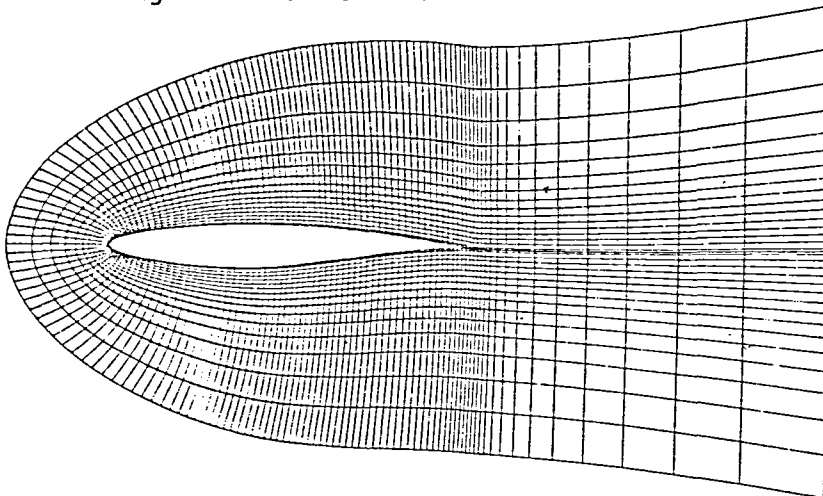


Fig 34 - Calculation of the RAE 2822 in a subcritical flow.



RAE2822 CAS08 - JCF01L8 - 181X27

Fig 35 - Mesh in a supercritical transonic flow with symmetrical wake.

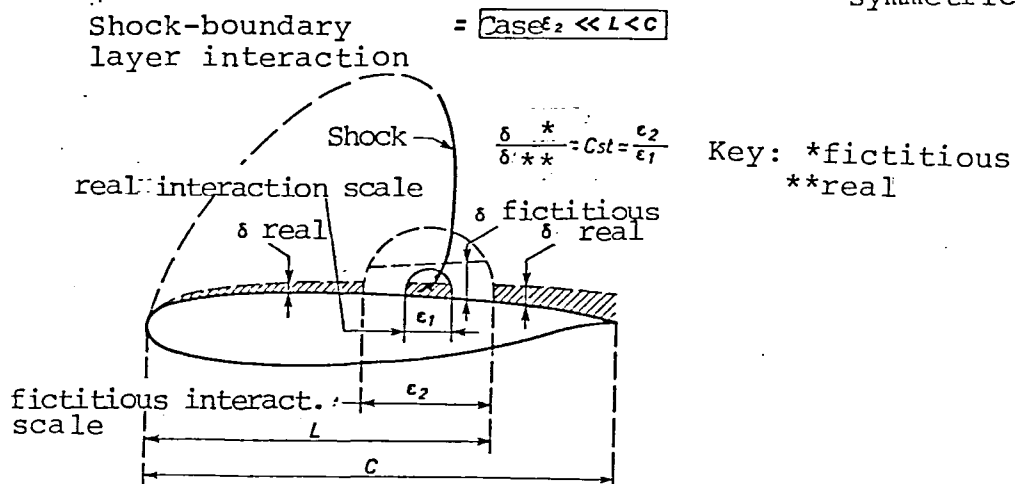


Fig 36 - Approximate calculation of the shock - boundary layer interaction if $\epsilon_2 \ll L < C$.

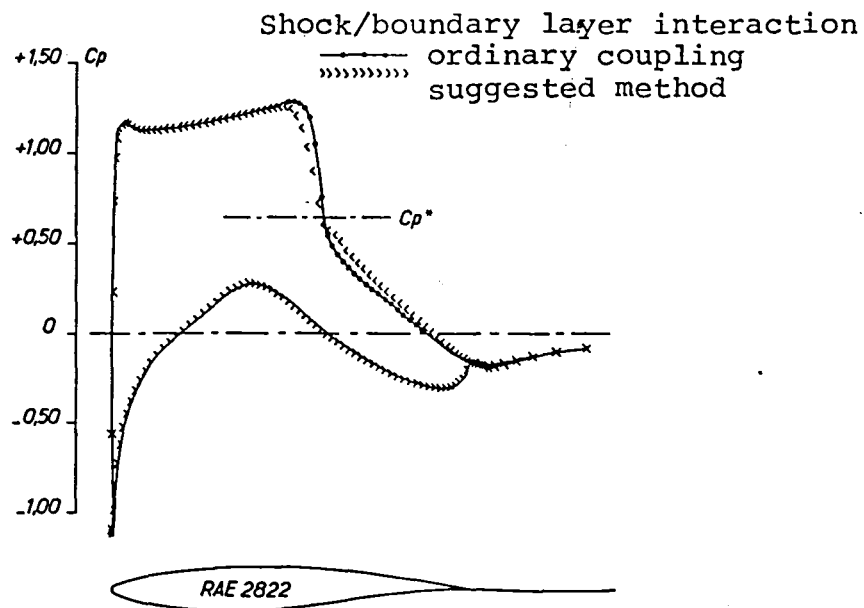


Fig 37 - Effect of the shock/boundary layer interaction.

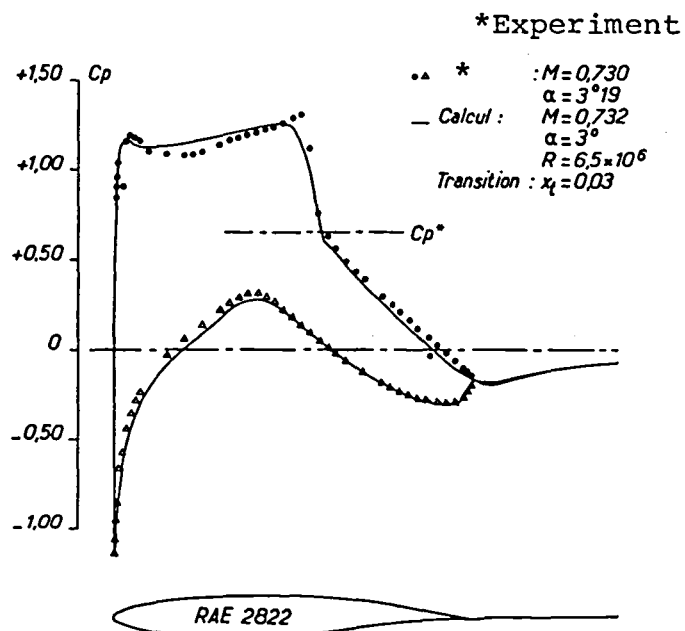
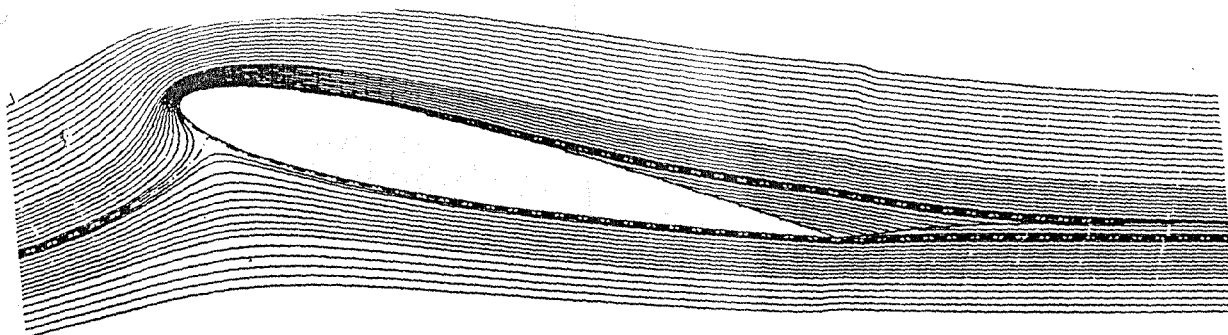
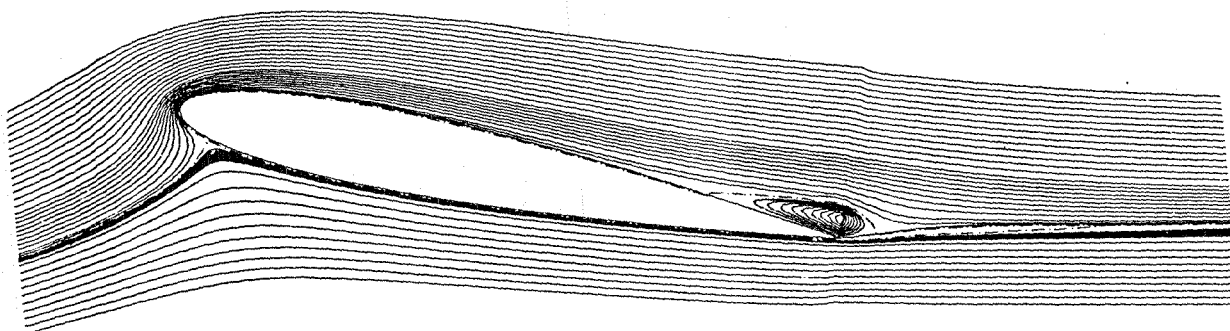


Fig 38 - Calculation of the RAE 2822 in a supercritical flow.



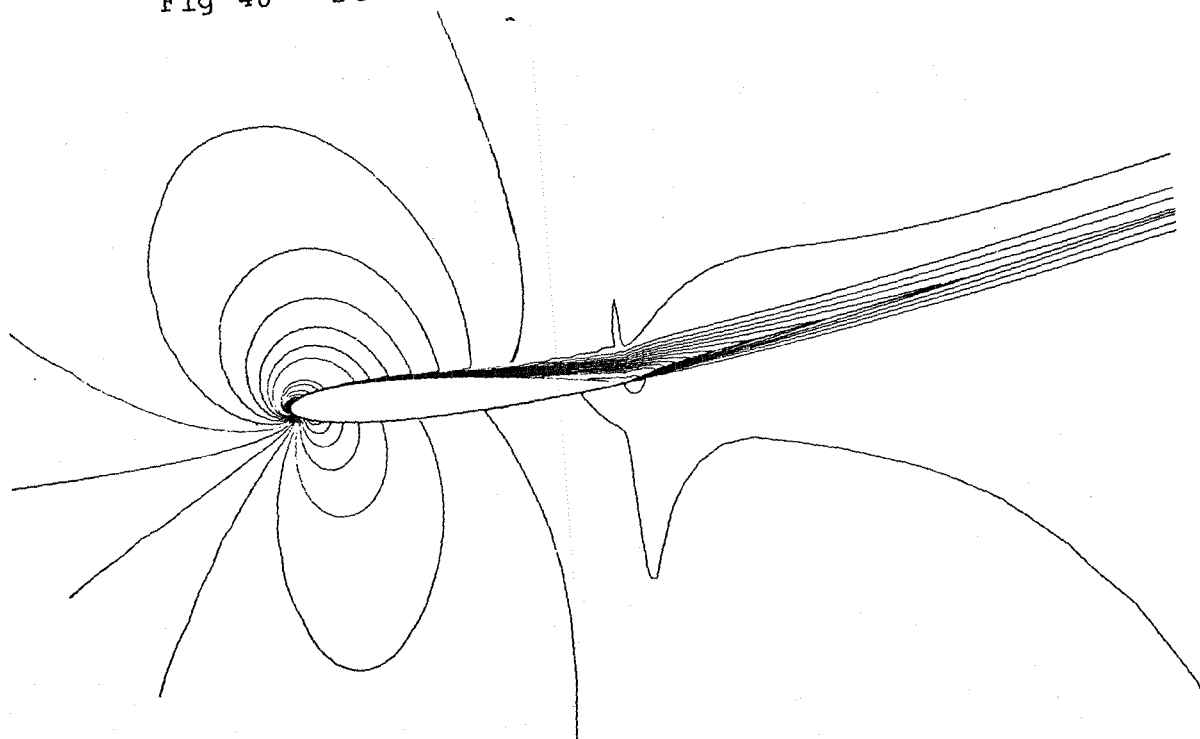
NACA 0012 ($M=0,116$, $\alpha=16^\circ$, $R=2 \times 10^6$).

Fig 39 - Streamlines in the inviscid flow - NACA airfoil 0012



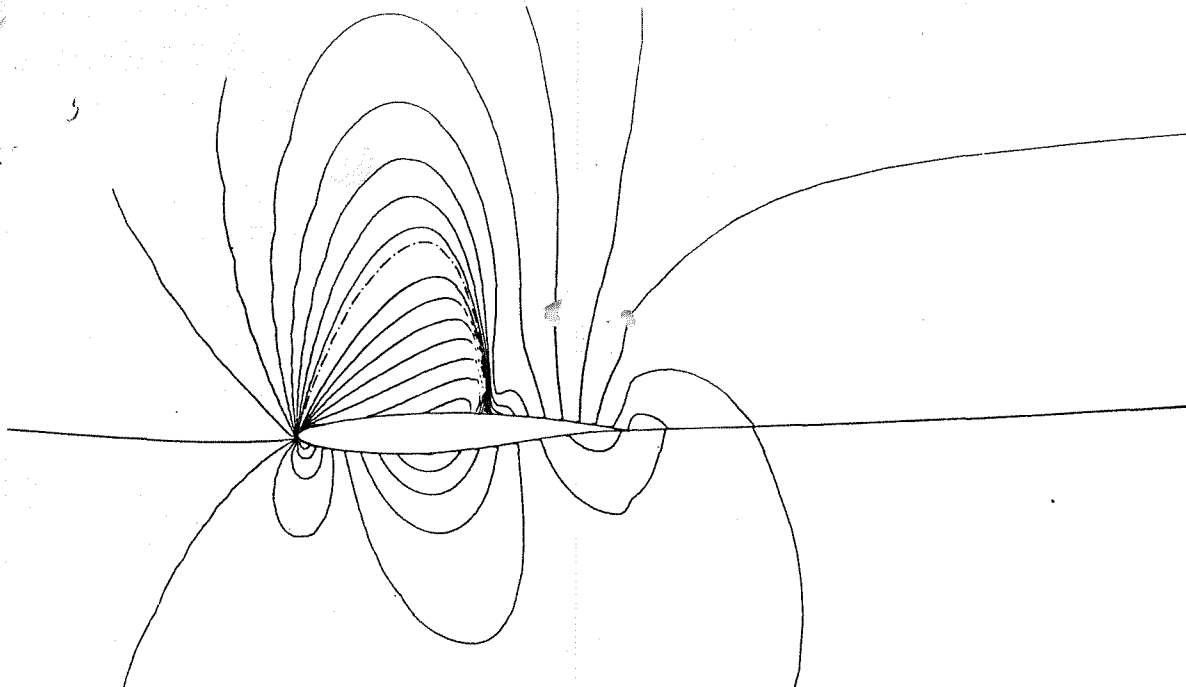
($M=0,116$, $\alpha=16^\circ$, $R=2 \times 10^6$).

Fig 40 - Streamlines in a viscous flow - NACA airfoil 0012



Profil NACA 0012 ($M=0,116$, $\alpha=16^\circ$, $R=2 \times 10^6$).

Fig 41 - Isomach lines in a viscous flow NASA airfoil 0012



Profil RAE 2822 supercritique ($M = 0,732$, $\alpha = 3^\circ$, $R = 6,5 \times 10^6$).

Fig 42 - Isomach lines in an inviscid flow - RAE supercritical 2822 airfoil

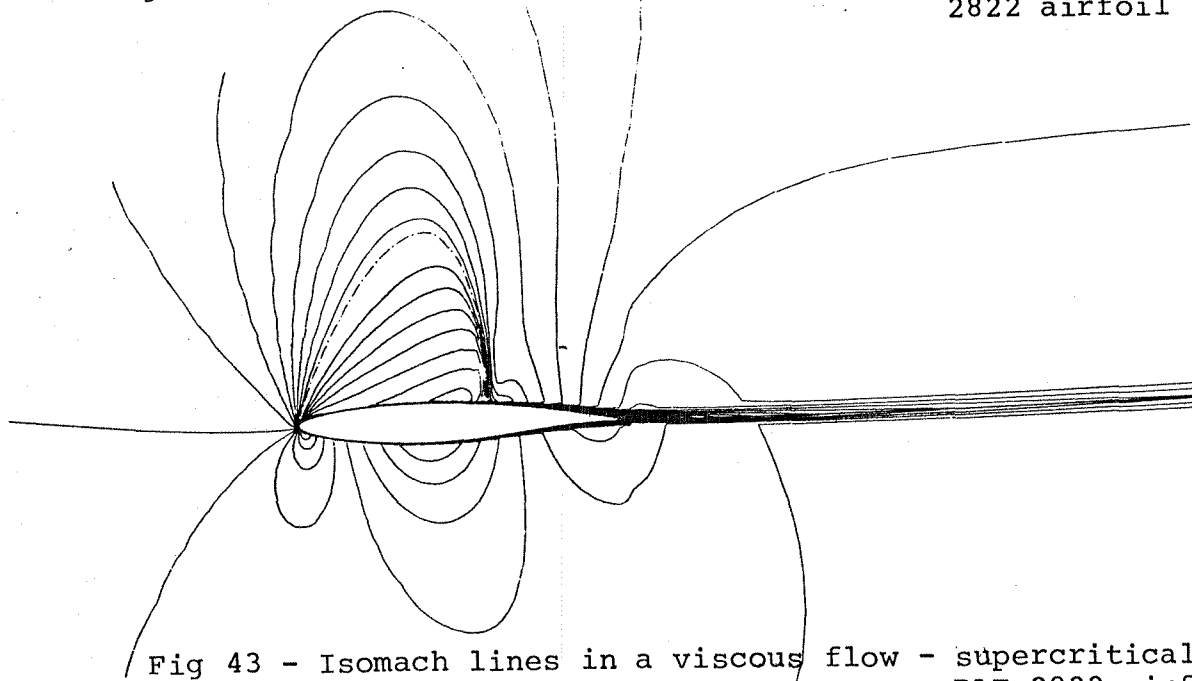
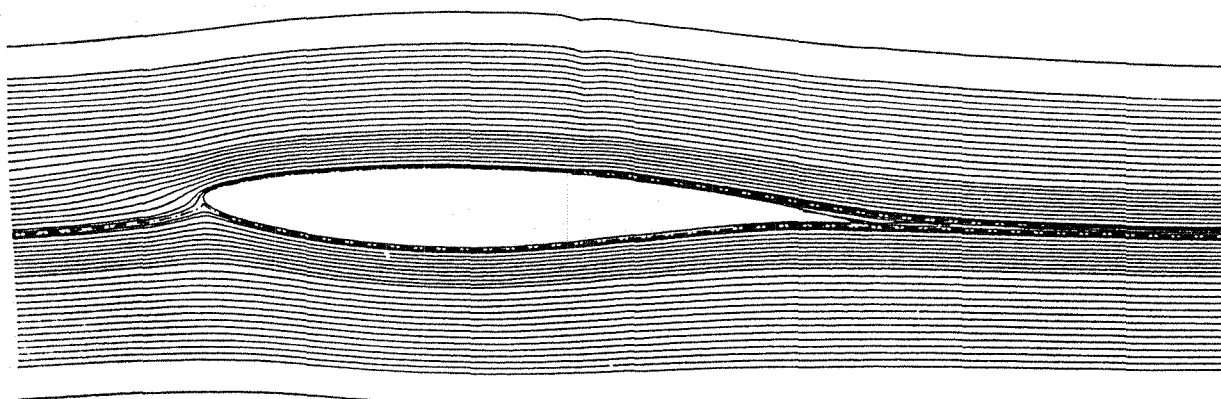


Fig 43 - Isomach lines in a viscous flow - supercritical RAE 2822 airfoil

Profil RAE 2822 supercritique ($M = 0,732$, $\alpha = 3^\circ$, $R = 6,5 \times 10^6$).



Profil RAE 2822 ($M = 0,732$, $\alpha = 3^\circ$, $R = 6,5 \times 10^6$).

Fig 44 - Streamlines in an inviscid flow

End of Document